

EFFECT OF OXIDATIVE STRESS ON MICROGLIAL ACTIVATION AND IRON  
ACCUMULATION



A Thesis Submitted in Partial Fulfillment of the Requirements  
for the Degree of Master of Science in Medical Sciences

Common Course

FACULTY OF MEDICINE

Chulalongkorn University

Academic Year 2019

Copyright of Chulalongkorn University

ผลของภาวะเครียดออกซิเดชันต่อภาวะภูการะตุ้นของเซลล์ไมโครเกลียและการสะสมของเหล็ก



วิทยานิพนธ์นี้เป็นส่วนหนึ่งของการศึกษาตามหลักสูตรปริญญาวิทยาศาสตรมหาบัณฑิต  
สาขาวิชาวิทยาศาสตร์การแพทย์ ไม่สังกัดภาควิชา/เทียบเท่า  
คณะแพทยศาสตร์ จุฬาลงกรณ์มหาวิทยาลัย  
ปีการศึกษา 2562  
ลิขสิทธิ์ของจุฬาลงกรณ์มหาวิทยาลัย



รัตนากร สันตะवालิม : ผลของภาวะเครียดออกซิเดชันต่อภาวะถูกกระตุ้นของเซลล์ไมโครเกลียและการสะสมของเหล็ก. ( EFFECT OF OXIDATIVE STRESS ON MICROGLIAL ACTIVATION AND IRON ACCUMULATION) อ.ที่ปรึกษาหลัก : รศ. ดร.พุลลาภ ชีพสุนทร, อ.ที่ปรึกษาร่วม : ผศ. ดร.ชาลิสา หลุยเจริญ ชีพสุนทร

เซลล์ไมโครเกลียเป็นเซลล์ค้ำจุนในระบบประสาทส่วนกลาง ทำหน้าที่เสมือนเซลล์ภูมิคุ้มกันของสมอง เซลล์ไมโครเกลียในสถานะถูกกระตุ้นจะมีการเพิ่มจำนวนมากขึ้นในสมองที่มีการเสื่อมตามอายุขัยและจะพบมากขึ้นในสมองของผู้สูงอายุที่เป็นโรคความเสื่อมทางระบบประสาท โดยพบว่าเซลล์ไมโครเกลียที่ถูกกระตุ้นเหล่านี้มีการสะสมธาตุเหล็ก ซึ่งธาตุเหล็กนี้จะทำให้เกิดการสร้างอนุพันธ์ออกซิเจนที่ว่องไวผ่านทางปฏิกิริยาเฟนตัน ดังนั้นการเพิ่มจำนวนของเซลล์ไมโครเกลียที่ถูกกระตุ้นและมีธาตุเหล็กสะสมภายในเซลล์ จึงถูกมองว่าเป็นปัจจัยคุกคามหนึ่งซึ่งส่งผลต่อการอยู่รอดของเซลล์ประสาท แต่อย่างไรก็ตามสาเหตุที่ทำให้เซลล์ไมโครเกลียที่ถูกกระตุ้นมีการสะสมของธาตุเหล็กยังไม่เป็นที่ทราบ ผู้วิจัยจึงตั้งสมมติฐานว่าระดับความเครียดออกซิเดชัน ที่เพิ่มขึ้นในสมองที่มีการเสื่อมตามอายุขัยและในโรคความเสื่อมทางระบบประสาท อาจจะเป็นสาเหตุสำคัญที่จะชักนำให้เซลล์ไมโครเกลียมีการสะสมธาตุเหล็กมากขึ้น วัตถุประสงค์ของการศึกษานี้คือเพื่อศึกษาผลของความเครียดออกซิเดชันต่อการสะสมของธาตุเหล็กและภาวะการถูกกระตุ้นของเซลล์ไมโครเกลีย โดยทำการทดลองเพาะเลี้ยงเซลล์ไมโครเกลียภายใต้ภาวะเครียดออกซิเดชันโดยตรง และภายใต้ภาวะเครียดออกซิเดชันที่ผ่านทางเซลล์แอสโตไซด์ ผลการศึกษาพบว่าการกระตุ้นด้วยภาวะเครียดออกซิเดชันโดยตรงไม่ทำให้เซลล์ไมโครเกลียมีการสะสมของธาตุเหล็ก ในขณะที่การกระตุ้นด้วยภาวะเครียดออกซิเดชันที่ผ่านทางเซลล์แอสโตไซด์ทำให้เซลล์ไมโครเกลียมีการสะสมของธาตุเหล็กและทำให้เซลล์อยู่ในสภาวะถูกกระตุ้น โดยมีการเพิ่มขึ้นของตัวบ่งชี้ภาวะการถูกกระตุ้นของเซลล์ไมโครเกลีย ทั้งการแสดงออกของ ferritin เพิ่มขึ้น, สารกระตุ้นการอักเสบ (IL-1 $\beta$ , IL-6, and TNF- $\alpha$ ) เพิ่มขึ้น, อนุพันธ์ออกซิเจนที่ว่องไวเพิ่มขึ้น และความต่างศักย์ของเมมเบรนไมโทคอนเดรียลดลง นอกจากนี้เซลล์ไมโครเกลียยังพบการสะสมของธาตุเหล็กผ่านทาง การเพิ่มขึ้นของโปรตีนที่นำธาตุเหล็กเข้า DMT1 และการลดลงของโปรตีนที่นำธาตุเหล็กออก FPN โดยสรุปแล้วการสะสมของธาตุเหล็กในเซลล์ไมโครเกลียเป็นผลมาจากภาวะเครียดออกซิเดชันที่ผ่านทางเซลล์แอสโตไซด์ แต่ไม่ได้มีผลมาจากภาวะเครียดออกซิเดชันโดยตรง

สาขาวิชา      วิทยาศาสตร์การแพทย์  
ปีการศึกษา     2562

ลายมือชื่อนิสิต .....  
ลายมือชื่อ อ.ที่ปรึกษาหลัก .....  
ลายมือชื่อ อ.ที่ปรึกษาร่วม .....

# # 6074077230 : MAJOR MEDICAL SCIENCES

KEYWORD: Microglia, Oxidative stress, Iron accumulation

Rattanakorn Suntawalimp : EFFECT OF OXIDATIVE STRESS ON MICROGLIAL ACTIVATION AND IRON ACCUMULATION. Advisor: Assoc. Prof. POONLARP CHEEPSUNTHORN, Ph.D. Co-advisor: Asst. Prof. CHALISA LOUICHAROEN CHEEPSUNTHORN, Ph.D.

Microglia are the glial cell in the central nervous system. They function as resident immune cells in the brain. Microglial activation was an increase in the normal aged brain and also more found in the aged brain with neurodegenerative disease. Activated microglial were found iron accumulation leading to increase ROS generation via the Fenton reaction. Therefore, the increase of microglial activation and iron accumulation is vulnerable to neuronal survival. However, the cause of iron accumulation in the activated microglia still unknown. This study hypothesized that oxidative stress which increases in the aged and neurodegenerative disease brain may cause microglial activation and also accumulate iron. The aim of this study was to investigate the effect of oxidative stress to iron accumulation and microglial activation by exposing in the directly oxidative stress and the indirectly oxidative stress via astrocyte conditioned medium. These data demonstrated that the directly expose oxidative stress to microglia did not induce iron deposition while the indirectly oxidative stress via H<sub>2</sub>O<sub>2</sub> astrocyte conditioned medium induced iron deposition and microglial activation. These microglia evidenced the marker of activated microglia as increased ferritin expression, elevated pro-inflammatory cytokines (IL-1 $\beta$ , IL-6, and TNF- $\alpha$ ), increased ROS level, and decreased mitochondria membrane potential. In addition, iron accumulation was found in these microglia by interrupting the iron import protein (DMT1), and the iron export protein (FPN). In conclusion, iron accumulation in microglia is a consequence of indirect oxidative stress through astrocyte, not the result of direct oxidative stress.

Field of Study: Medical Sciences

Student's Signature .....

Academic Year: 2019

Advisor's Signature .....

Co-advisor's Signature .....

## ACKNOWLEDGEMENTS

I would like to thank the following people for their encouragement and all guidance thoroughly in my master's degree study. This thesis would not have been possible without their support. First of all, I would like to express my grateful thanks to my advisor Associate Professor Dr. Poonlarp Cheepsunthorn for his suggestions, patience, and all the support during my study. He always challenges me to think more deeply and make decisions by myself. I deeply appreciate what I learned so much from him, not only theoretical knowledge but also attitudes in life, leading me to grow up and thinking better. Further, I would like to thank my co-advisor, Assistant Professor Dr. Chalisa Louicharoen Cheepsunthorn for her kindly advice and all help. I sincerely apologize for any of my mistakes.

In addition, my gratitude is also extended to Professor Vilai Chentanez who was the chairman of the thesis defense, Assistant Professor Dr. Wacharee Limpanasithikul who was my thesis committee, and Assistant Professor Dr. Pattama Leewanich who was the external committee from the Department of Pharmacology, Faculty of Medicine, Srinakharinwirot University, for their valuable advice. I am also thankful to the educational program officer, Miss Apinya Butlee for her great recommendations during I was here.

I also would like to express my warm gratitude to members of 828 laboratory for their counseling, teaching me in laboratory skills, and always supported me.

Finally, I would like to special thanks to the most important of my life, my family including my father, mother, elder brother, and elder sister for their understanding, love, and always stand beside me.

This work was funded by the scholarship from the Graduate School, Chulalongkorn University to commemorate the 72nd anniversary of his Majesty King Bhumibol Adulyadej is gratefully acknowledged.

Rattanakorn Suntawalimp



จุฬาลงกรณ์มหาวิทยาลัย  
**CHULALONGKORN UNIVERSITY**

## TABLE OF CONTENTS

	Page
ABSTRACT (THAI).....	iii
ABSTRACT (ENGLISH).....	iv
ACKNOWLEDGEMENTS .....	v
TABLE OF CONTENTS .....	vii
LIST OF TABLES.....	x
LIST OF FIGURES .....	xi
LIST OF ABBREVIATIONS .....	1
CHAPTER I INTRODUCTION .....	5
1.1 Background and Rationale.....	5
1.2 Research Questions.....	6
1.3 Objectives.....	6
1.4 Hypotheses.....	6
1.5 Keywords .....	6
1.6 Research Design.....	6
1.7 Conceptual Framework.....	7
1.8 Benefits of study .....	7
CHAPTER II LITERATURE REVIEW .....	8
2.1 Neurodegenerative changes.....	8
2.1.1 Structural changes.....	8
2.1.2 Functional changes.....	8
2.1.3 Cellular and molecular changes.....	9



2.2 Neurodegenerative changes and oxidative stress .....	10
2.3 Oxidative stress.....	11
2.3.1 Exogenous sources of ROS.....	11
2.3.2 Endogenous sources of ROS.....	12
2.3.3 Antioxidant pathway .....	14
2.4 Brain Iron Homeostasis.....	15
2.5 Iron regulation by IRE/IRP pathway .....	17
2.6 Microglia .....	19
2.6.1 Role of microglia.....	20
2.6.2 Microglia activation.....	21
2.6.2.1 Stimulators of microglial activation.....	23
2.6.3 Cytotoxic of activated microglia .....	24
2.6.4 Microglia and iron .....	24
2.7 Microglia and Neurodegenerative diseases.....	25
CHAPTER III MATERIALS AND METHODS .....	27
3.1 Reagents.....	27
3.2 Experimental design .....	28
3.3 Cell culture and treatment.....	28
3.4 Cell viability by MTT assay.....	29
3.5 Ferric iron detection by Perls' Prussian blue staining with DAB enhancement.	29
3.6 Intracellular iron detection by Calcein AM assay.....	29
3.7 Western blotting.....	30
3.8 Immunofluorescence assay .....	30
3.9 RNA isolation and Quantitative Real-time Polymerase Chain Reaction (q-PCR)	31

3.10 Enzyme-linked immunosorbent assay (ELISA) .....	31
3.11 Intracellular Reactive Oxygen Species (ROS) assay .....	33
3.12 Mitochondrial Membrane Potential (MMP) $\Delta\Psi_m$ .....	33
3.13 Statistical analysis .....	34
CHAPTER IV RESULTS .....	35
4.1 Iron accumulation was observed in microglia induced by H <sub>2</sub> O <sub>2</sub> ACM. ....	35
4.2 Microglia were activated by H <sub>2</sub> O <sub>2</sub> ACM.....	38
4.3 Iron homeostasis in microglia was altered by H <sub>2</sub> O <sub>2</sub> ACM.....	43
4.4 The increasing of ROS and mitochondrial dysfunction was shown in microglia induced by H <sub>2</sub> O <sub>2</sub> ACM.....	46
CHAPTER V DISCUSSION AND CONCLUSION.....	48
REFERENCES .....	52
APPENDIX.....	64
VITA.....	68

## LIST OF TABLES

	Page
Table 1: The secretions from microglia .....	22
Table 2: Protein aggregations in neurodegenerative diseases.....	26
Table 3: Specific primers.....	32



## LIST OF FIGURES

	Page
Figure 1: Production of ROS .....	12
Figure 2: Mitochondrial ROS production .....	13
Figure 3: The diagram of the iron transport mechanism.....	18
Figure 4: IRE-IRP pathway .....	19
Figure 5: Iron transport pathway in microglia .....	25
Figure 6: Mechanism of ROS assay.....	33
Figure 7: Relative microglia cell viability determined by MTT assay. ....	35
Figure 8 Directly exposed oxidative stress did not induce iron accumulation in microglia. ....	36
Figure 9: Indirectly exposed oxidative stress via astrocyte conditioned medium induced iron accumulation in microglia. ....	37
Figure 10: Indirectly exposed oxidative stress via astrocyte conditioned medium induced microglia activation. ....	39
Figure 11: Ferritin light chain protein was increased in the H <sub>2</sub> O <sub>2</sub> astrocyte conditioned medium group.....	40
Figure 12: Indirectly exposed oxidative stress via astrocyte conditioned medium microglia induced microglia increased the expressions of proinflammatory cytokines. ....	42
Figure 13: Indirectly exposed oxidative stress via astrocyte conditioned medium altered iron homeostasis in microglia. ....	45
Figure 14: Indirectly exposed oxidative stress via astrocyte conditioned medium increased ROS levels and decreased mitochondria membrane potential in microglia. ....	47



จุฬาลงกรณ์มหาวิทยาลัย  
**CHULALONGKORN UNIVERSITY**

## LIST OF ABBREVIATIONS

°C	degree celsius
µg	Microgram
µl	Microliter
·OH	hydroxyl radicals
8-OHdG	8-Hydroxy-2-deoxyguanosine
ACM	astrocyte conditioned medium
AD	Alzheimer's disease
ANOVA	analysis of variance
BBB	blood brain barrier
BCA	bicinchoninic acid assay
BDNF	brain-derived neurotrophic factor
BSA	bovine serum albumin
Calcein-AM	Calcein acetoxymethyl ester
Cat	Catalase
cDNA	complementary-deoxyribonucleic acid
CM-H2DCFDA	5-(and-6)-chloromethyl-2',7'-dichlorodihydrofluorescein diacetate
CNS	central nervous system
CSF	cerebrospinal fluid
CX3CL1	fractalkine ligand 1
CX3CR1	fractalkine receptor 1
DAB	3,3'-diaminobenzidine
DAPI	4',6-Diamidino-2-Phenylindole, Dihydrochloride
DCF	2'-7'dichlorofluorescein
DMT1	divalent metal transporter-1
DNA	deoxyribonucleic acid
ELISA	enzyme-linked immunosorbent assay

ER	endoplasmic reticulum
ETC	electron transport chain
Fe <sup>2+</sup>	ferrous
Fe <sup>3+</sup>	ferric
FPN	ferroportin
Ft-H	ferritin heavy subunits
Ft-L	ferritin light subunits
GFAP	glial acidic fibrillary protein
GPX	glutathione peroxidase
GSH	glutathione
GSH	glutathione
H <sub>2</sub> O <sub>2</sub>	hydrogen peroxide
H <sub>2</sub> O <sub>2</sub> ACM	H <sub>2</sub> O <sub>2</sub> (10 uM) astrocyte conditioned medium
HNE	4-hydroxy-2-nonenal
HRP	horseradish peroxidase
IFN- $\gamma$	interferon- $\gamma$
IGF1	insulin-like growth factor 1
IL-1 $\beta$	interleukin-1 $\beta$
IL-6	interleukin-6
IRE	iron-responsive element
IRP	iron regulatory protein
LIP	labile iron pool
LPS	lipopolysaccharide
LSD	least-Significant Difference
LTP	long-term potentiation
MCP-1	monocyte chemoattractant protein 1
MDA	malondialdehyde

MDC	macrophage-derived chemokine/CCL22
Mg	milligram
MHC II	major histocompatibility complex class II
Min	minute
MIP-1,2	macrophage inflammatory protein 1,2
ml	millilitre
mM	millimolar
MMP	mitochondria membrane potential
MRI	magnetic resonance imaging
NF- $\kappa$ B	nuclear factor -kappa B
NGF	nerve growth factor
nm	nanometer
NO	nitric oxide
NT3,4	neurotrophin-3,4
NTBI	nontransferrin-bound iron
O <sub>2</sub> <sup>-</sup>	superoxide
OH <sup>-</sup>	hydroxyl anions
PBS	phosphate buffered saline
PD	Parkinson's disease
PGE2	Prostaglandin E2
PMA	Phorbol 12-Myristate 13-Acetate
PRX	Peroxiredoxins
PSD95	postsynaptic density 95
PUFAs	polyunsaturated fatty acids
q-PCR	Quantitative Real-time Polymerase Chain Reaction
RNA	ribonucleic acid
ROS	reactive oxygen species



SDS-PAGE	sodium dodecyl sulfate-polyacrylamide gel electrophoresis
SEM	standard error of mean
SOD	superoxide dismutase
TBI	transferrin-bound iron
TBS-T	tris buffered saline with Tween-20
Tf	Transferrin
TfR	transferrin receptor
TGF- $\beta$	transforming growth factor $\beta$
TNF- $\alpha$	tumor necrosis factor alpha
UTR	untranslated region



# CHAPTER I

## INTRODUCTION

### 1.1 Background and Rationale

Microglia, constituting around 10% of all glial cells, function as a resident immune cell in the central nervous system. In physiological condition, microglia processes are continuous motion for surveying the brain microenvironment and searching for brain damage to form the first line of defense. (1, 2) Upon brain infection or injury, microglia would change morphology which reflects a highly activated state, and cell bodies enlargement while cell processes would be shortening. They also migrate to the injury site and secrete cytokine mediators to maintain homeostasis and promote neuronal survival.

Microglial activation was increased in normal aged brain and also more found in aged brain with neurodegenerative disease including Alzheimer's disease (AD) and Parkinson's disease (PD). Under microscope observation, activated microglial have found iron accumulation. Moreover, iron accumulation in microglia can increase the generation of ROS including hydroxyl radical ( $\text{OH}^{\bullet}$ ) via the Fenton reaction, which are involved in neuronal cell death by inducing the damage of membrane and DNA (3).

The in vitro study has revealed that activated microglia become more toxic to neuron when accumulating iron (4, 5). Thus, the increase of microglial activation and iron accumulation is vulnerable to neuronal survival. In line with the current concept that targeting to reduce or inhibit microglial activation which helps to alleviate neuronal damage in neurodegenerative disease. However, the cause of iron accumulation in the activated microglia has been unknown.

In this study, we hypothesize that oxidative stress which increase in the aged and neurodegenerative disease brain may cause microglial activation and also accumulate iron. We decided to induce oxidative stress by long term and low concentration of hydrogen peroxide. We investigated the iron accumulation, microglial activation markers and also determined iron homeostasis protein.

This study is beneficial to understand the mechanism of toxicity from microglia as found in neurodegenerative disease and also would be able to explore the novel strategies to prevent or relieve the toxicity of microglia in neurodegenerative disease with existing drugs.

## 1.2 Research Questions

- 1.2.1 Does oxidative stress induce iron accumulation in microglia?
- 1.2.2 Does oxidative stress induce microglial activation?
- 1.2.3 Does microglial activation induced by oxidative stress affect neurotoxicity?

## 1.3 Objectives

- 1.3.1 To investigate whether oxidative stress induced iron accumulation in microglia.
- 1.3.2 To determine whether oxidative stress induced microglial activation.
- 1.3.3 To examine the effect of oxidative stress in microglia induced neurotoxicity.

## 1.4 Hypotheses

Oxidative stress can induce iron accumulation and increase activation in microglia.

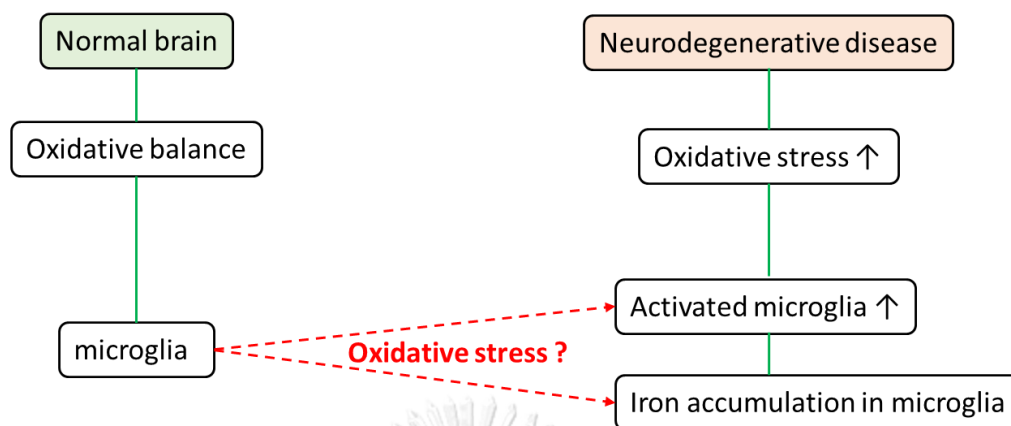
## 1.5 Keywords

- 1.5.1 Microglia
- 1.5.2 Oxidative stress
- 1.5.3 Iron accumulation
- 1.5.4 Neurodegenerative diseases

## 1.6 Research Design:

Experimental design

## 1.7 Conceptual Framework



## 1.8 Benefits of study

This study is beneficial for understanding the mechanism of activated microglia by oxidative stress. It might be useful for future research that find therapeutic strategy to inhibit microglial activation for reduce neuronal cell death and severity of neurodegenerative diseases.

## CHAPTER II

### LITERATURE REVIEW

#### 2.1 Neurodegenerative changes

Aging is a general process that leads to loss of physiological functions across an organism. The aging is the most risk factor in neurodegenerative disease including Alzheimer's disease (AD) and Parkinson's disease (PD) (6). Aging affects the brain change in structural, molecular and functional which are not specific to individual changes.

##### 2.1.1 Structural changes

In the aged brain, it has been found that the brain volume declines which predominant in the frontal cortex, temporal cortex, putamen, thalamus and nucleus accumbens (7). The volume loss is accompanied by increasing in ventricular volume and other cerebrospinal fluid (CSF) spaces. The magnetic resonance imaging (MRI) study shown a reduction in grey matter volume (8) while increasing white matter volume (9). Human brain volume from aged over 60 years old was declined 17 % lighter than brain from young adults (10). The brain shrinks with age occurred due to loss of dendrites, spines and myelin dystrophy, as well as the alterations in synaptic transmission (11). In addition, human older than 50 years old was 46 % decreased in spine number and density when compared with younger adult (7).

##### 2.1.2 Functional changes

Brain functions were alteration in cognition, speech, sleep, decision making, working and long term memory with age (12). Attention and memory function were the most affected in the elderly. Attention is important for being independent of activity daily living. The impairments of attention with age affect to daily activity especially driving performance. These impairments are significantly correlated with increased vehicle accidents in the elderly (13). Moreover, the elderly have an impairment of working memory. The functional neuroimaging studies have shown

that brain region activated areas especially in the prefrontal cortex are different between young and older adults (14). Also, it was found that cortical activities were decreased in the elderly and correlated with the decrease in working memory function (15).

### **2.1.3 Cellular and molecular changes**

The aged brain is related to changes in the levels of neurotransmitters, enzymes, hormones, and metabolism. The loss of dopaminergic neurons in frontal cortex and striatum and decreasing in binding affinity of dopamine receptors caused dopamine levels decline and been associated with declines in cognitive and motor performance (16). Serotonin levels also decrease with age and associate with the loss of synaptic plasticity and neurogenesis in the aged brain (17).

A cellular component in the brain consists of the neurons and glial cells which include astrocytes, oligodendrocytes, and microglial cells. The number of total neurons decreased by 9.5% from the age of 20 to 90 years. The neuronal loss was also found in subcortical regions around 67% with age-related (18). Furthermore, stereological quantification of glia in neocortical regions of old brains has suggested that the number of oligodendrocytes decreased but not of astrocyte and microglia in old human brains (19, 20). During aging, astrocytes as determined by glial acidic fibrillary protein (GFAP) positivity, shown a flat morphology and become more activated (21, 22). The increased expression of GFAP during aging may be enhanced to decrease synaptic functions (23). Similarly, microglia were increased activation and found in rodents, as well as in primates and humans. This activation was the most frequently reported by an age-dependent increase in major histocompatibility complex class II (MHC II) antigens (24, 25). The current study examined brain-wide gene expression patterns in the aging human brain. It found that glial specific gene expression was increased, while neuron-specific gene expression was decreased aligns with the decrease numbers of neurons. It implied that the gene of glial specific might be a good indicator of age better than neurons (26).

Moreover, the increase of iron accumulation has shown in the aged brain and also found in various regions that depend on the affected brain region of neurodegenerative disease (27). The iron accumulations are also affected on cognitive ability. The study of preclinical mild cognitive impairment (MCI) cases has been found that elevated iron in MCI cases when compared to normal cognitively aged-matched control cases. In addition, the accumulation of redox-active iron in glial cells has been found in MCI cases and tends to increase in cases with the severity of cognitive impairment (28). Nowadays, the study of iron deposition in the brain may be providing strategies to prevent the brain age-related diseases.

Excessive generation of free radicals and the reduction of antioxidant enzymes that cause oxidative stress were associated with aging. Oxidative stress can damage cells and DNA leading to functional declines in aging. The brain is the organ that highly susceptible to oxidative stress.

## **2.2 Neurodegenerative changes and oxidative stress**

Aging is the biggest risk factor in several diseases including neurodegenerative diseases. Nowadays, it is widely found that oxidative stress was increased in the brain with age. The brain is the most vulnerable to the damaging effect of oxidative stress (29, 30) because the brain has more high concentrations of polyunsaturated fatty acids (PUFAs) when compared to other tissues and require the highest amount of oxygen to produce energy which can cause susceptible to lipid peroxidation. The brain also contains a high level of iron and ascorbate enhancing membrane lipid peroxidation. Moreover, there is no high antioxidant defenses in the brain when compared to other organs. It has a lower activity of glutathione peroxidase (GPx) and catalase (Cat) (31).

In aging brain, brain functions were declined which related to the increase of oxidative stress and the decreased of the antioxidant defense mechanism. As previous studies assessing the increased of the oxidative damage biomarkers in brain

aging and other neurodegenerative diseases which are included the biomolecules like lipids, proteins, and DNA (32). The malondialdehyde (MDA) and 4-hydroxy-2-nonenal (HNE) as the group of aldehyde markers of lipid peroxidation were found highly in neurons and astrocytes with age (33). The study in the post-mortem brain of aged human observed the high levels of 8-Hydroxy-2-deoxyguanosine (8-OHdG), as a hydroxyl radical-damaged guanine nucleotide the marker of oxidative DNA alteration (34). In addition, the aged human cerebral cortex increased the protein oxidation which measured by the levels of protein carbonyl groups (35).

### 2.3 Oxidative stress

Regulated systems in living organisms must keep reactive oxygen species (ROS) at very low levels that control both production and elimination resulting in balance certain steady-state ROS levels. Nonetheless, this balance can be disturbed resulting in excessive accumulation of ROS and this condition is known as oxidative stress. This condition is caused by several reasons such as the increase level of ROS production, lack of reserves of low molecular mass antioxidants, antioxidant enzymes are inactive, the production of antioxidant enzymes and low molecular mass antioxidants are decreased, and combinations of two or more from those factors in above (36).

Reactive oxygen species (ROS) are reactive molecules derived from oxygen with one unpaired electron resulting in short-lived and highly reactive. The common ROS and their productions are shown in figure 1. It is generated by various exogenous and endogenous sources (37, 38).

#### 2.3.1 Exogenous sources of ROS

The ROS can be generated by the various of exogenous sources including, ionizing radiation: exposure to gamma irradiation can produce radical and non-radical species, nonionizing radiation: exposure to ultraviolet (UV), UV-C (<290 nm), UV-B (290–320 nm), and UV-A (320–400 nm) can generate various ROS including  $O_2$ ,  $H_2O_2$ ,



and  $\bullet\text{O}_2$  radicals, Environmental toxins: Air pollution such as car exhaust, cigarette smoke, and industrial contaminants, and drugs: action mechanism of some drug is mediated via ROS production.

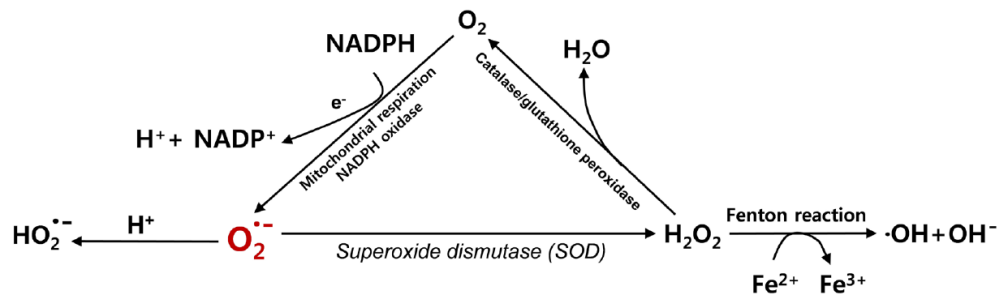


**Figure 1: Production of ROS**

The superoxide ( $\text{O}_2^{\cdot-}$ ) is both created from  $\text{O}_2$ , a by production from respiratory chain complex of mitochondria, and from NADPH oxidase. Then,  $\text{O}_2^{\cdot-}$  transforming into hydrogen peroxide ( $\text{H}_2\text{O}_2$ ) by superoxide dismutase (SOD) and transformed into other ROS including hydroxyl anions ( $\text{OH}^-$ ) and hydroxyl radicals ( $\cdot\text{OH}$ ) (39).

### 2.3.2 Endogenous sources of ROS

#### 1) Mitochondrial ROS production

The mitochondrion is the primary source of ROS production in most cells. The mitochondrial respiratory chain complexes are the main ROS. Mitochondrial electron transport chain (ETC) consists of five component complexes including Complex I (the NADH-coenzyme Q reductase or NADH dehydrogenase), Complex II (succinate dehydrogenase), Complex III (coenzyme Q-cytochrome c reductase), Complex IV (cytochrome C oxidase) and Complex V (ATP synthase). The major site for ROS production is within respiratory complexes I and III. ROS is generated from the leakage of electrons in the form of superoxide ( $\text{O}_2^{\cdot-}$ ). Complex I stimulate electron from NADH transfers to CoQ. Complex II is the reduction of CoQ and lowers generated ROS than complex I. Complex III induces electrons from  $\text{CoQH}_2$  transfer to cytochrome c via Q cycle. Mitochondrial ROS production is shown in figure 2.

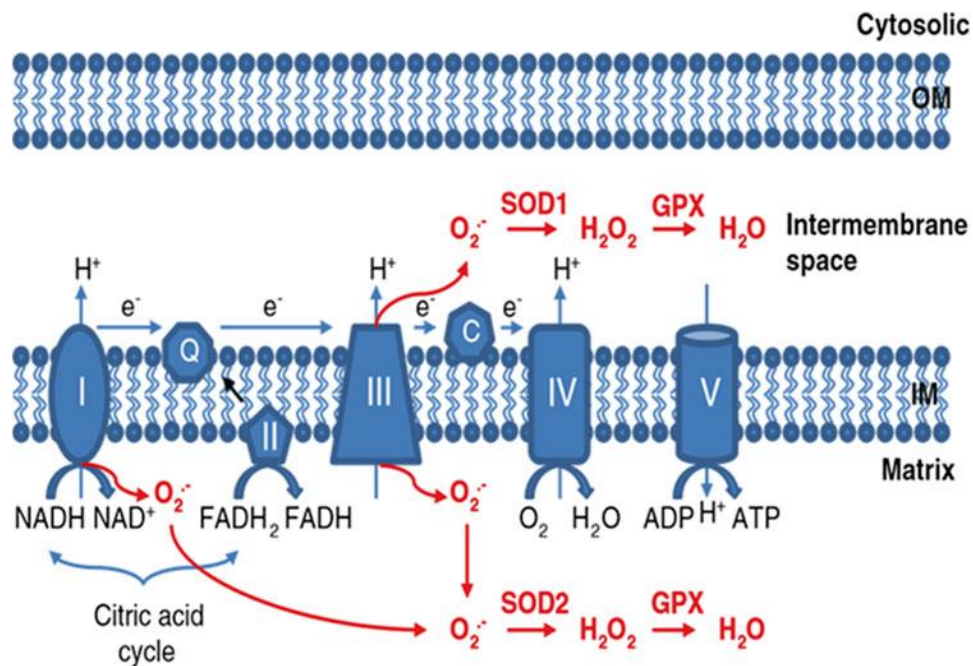


**Figure 2: Mitochondrial ROS production**

ROS is generated from the leakage of electrons (e<sup>-</sup>) in the form of superoxide (O<sub>2</sub><sup>-</sup>) in complex I and III. Superoxide dismutase 1 (SOD1) in the intermembrane space and SOD2 in the matrix causes O<sub>2</sub><sup>-</sup> transform into H<sub>2</sub>O<sub>2</sub>. Then, H<sub>2</sub>O<sub>2</sub> transforms into water (H<sub>2</sub>O) by glutathione peroxidase (GPX). (38)

## 2) Endoplasmic reticulum (ER) ROS production

The endoplasmic reticulum (ER) mainly involved in protein folding and lipid biosynthesis. ER produces ROS by two mechanisms: 1) during the transfer of electrons from protein thiol to oxygen molecular, ROS are produced as a by-product, 2) generated by protein misfolding.

## 3) Peroxisomes ROS production

Peroxisomes can generate the majority of H<sub>2</sub>O<sub>2</sub>. It also has catalases that convert H<sub>2</sub>O<sub>2</sub> to water and oxygen for protecting the cell from ROS accumulation. When catalases reducing caused by peroxisomes damaged, the H<sub>2</sub>O<sub>2</sub> levels in the cytosol were increased resulting in oxidative stress.

### 2.3.3 Antioxidant pathway

Cellular ROS levels are regulated by the defense mechanisms of antioxidant enzymes and small-molecule antioxidants (39).

#### 1) Superoxide dismutase (SOD)

SOD is a significant role in catalyzing the breakdown of superoxide ( $O_2^-$ ) that highly reactive to hydrogen peroxide ( $H_2O_2$ ) and oxygen which are less reactive. Isoforms of SOD are including cytosolic copper/zinc-SOD (SOD1), mitochondrial manganese SOD (SOD2), and extracellular SOD (SOD3). SOD1 is the main function to remove  $O_2^-$  in the cytosol, while the elimination of  $O_2^-$  in mitochondria is the function of SOD2.

#### 2) Glutathione peroxidases (GPX)

GPX functions to catalyze the reduction of  $H_2O_2$  and lipid peroxides utilizing GSH as an electron donor. In mammals, there are five different isoforms including glutathione peroxidases (GPX1-4 and 6) and three nonselenium congeners (GPX 5, 7 and 8). The antioxidant function of GPXs depends on each isoform and location in the cells. The main antioxidant enzymes in the brain are GPX1 that particularly express in microglia but not in neurons.

#### 3) Catalase (Cat)

Catalase functions to the conversion of  $H_2O_2$  to water and oxygen which using iron or manganese as a cofactor. The higher levels of  $H_2O_2$  are causes increasing the catalase activity.

#### 4) Peroxiredoxins (PRX)

PRX, thiol-specific peroxidases are responsible for catalyzing the reduction of  $H_2O_2$  as well as other organic hydroperoxides and peroxyxynitrite. The 90% of mitochondrial  $H_2O_2$  and almost 100% of cytoplasmic  $H_2O_2$  are reduced by PRX.

#### 5) Glutathione (GSH)

GSH is synthesized by the tripeptide from glutamate, cysteine, and glycine. It functions to protect the cell against oxidative stress. GSH is responsible for two

reactions including, non-enzymatic reaction which its reduced form reacts with  $O_2^-$  and  $\cdot OH$  for reduction of ROS, and the GPX reaction, GSH act as the electron donor for the reduction of peroxides. ROS oxidizes GSH which generates glutathione disulfide and the final product of GPX reactions.

In addition, the glutathione disulfide reacts with glutathione reductase that transfers electrons from NADPH to glutathione disulfide which regenerated the GSH. The most studies reported that oxidative stress induced apoptotic cell and DNA damage were reduced by GSH (40, 41)

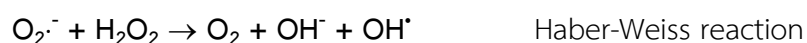
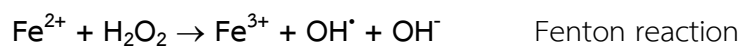
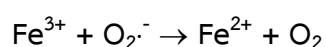
## 6) Vitamin E and C

Vitamin E, a lipid-soluble antioxidant, is involved in the reduction of the effects from peroxide and protect against lipid peroxidation in cell membranes. Vitamin C, a water-soluble antioxidant, can remove the free radicals by electron transfer. It also is the cofactor for antioxidant enzymes (42).

The brain contains a high level of iron which is vulnerable to oxidative damage. In addition, iron accumulation was found in aged and neurodegenerative disease brain. Therefore, the regulation of iron metabolism in the brain is crucial to understanding.

### 2.4 Brain Iron Homeostasis

Neurological functions are regulated by many proteins that required iron as the cofactor element. For example, tyrosine hydroxylase as the non-haem iron enzyme is involved in dopamine synthesis. Moreover, it involved in the synthesis of myelin that is necessary for brain function (43). While several studies found that increasing iron accumulates in the brain with age (27, 44) and can cause oxidative stress resulting in neurodegeneration (45, 46). Free iron can toxic to the cell by catalyzing the ROS generation ( $\cdot OH$ ,  $OH^-$ ) via the Fenton reaction as shown:



Iron metabolism is regulated by iron-related proteins including iron uptake, transportation, and storage proteins that controlled by iron at the cellular and systemic levels. (47). Iron metabolisms of the brain are acquired through a transport mechanism at the blood brain barrier (BBB) which transports iron across the endothelial cells into the brain. Transferrin (Tf) binding to its receptor (TfR) at the lumen of the brain microvasculature facilitates iron uptake through the endocytosis pathway. It affects Tf release ferric ( $\text{Fe}^{3+}$ ) in the acidic endosome. Then, it reduces to ferrous ( $\text{Fe}^{2+}$ ) and export from the endosome via divalent metal transporter-1 (DMT1). The iron is utilized for essential metabolic processes and the excess is stored in the complex of ferritin at cytosolic or is released outside the cell via ferroportin (FPN). Interestingly, Tf-TfR complex levels are lower than the levels in the systemic circulation but the non-Tf-bound iron (NTBI) levels are relatively high. Therefore, neurons and other cells in the brain received iron from NTBI which is the main source of iron. Ferritin is another source of iron that plays a crucial role in brain iron homeostasis (48). The ferritin can store iron up to 4500 atoms and is consists of 24 subunits including heavy (H) and light (L) subunits. Their subunits have different functions. Ferritin H (Ft-H) subunit function as a ferroxidase enzyme, catalyzes the oxidation of  $\text{Fe}^{2+}$  to  $\text{Fe}^{3+}$  which associated with stress responses, while ferritin L (Ft-L) subunit facilitates mineralization and stabilizes the ferritin complex structure which associated with iron storage in a long-term (49, 50). In the brain, the oligodendrocyte is the most common cell type that stained for iron in normal conditions (51). The ferritin is expressed in brain cells including neurons, microglia, and oligodendrocytes. Thus, these cells have functional to store iron. Moreover, the relative abundance of Ft-H and Ft-L depends on the cell type. In the neurons express mostly Ft-H, microglia express mostly Ft-L and oligodendrocytes express similar amounts of both subunits. The expression of ferritin in astrocyte was lower than other cell, indicating that these cells stored not highly iron level (52, 53).

## 2.5 Iron regulation by IRE/IRP pathway

The iron regulatory protein (IRP) and iron-responsive element (IRE) signaling pathway is posttranscriptional iron homeostasis regulation in response to intracellular iron levels which associates iron absorption, export, utilization, and storage (54). The IRE is 30 nucleotide long RNA motifs in a stem loop structure at the untranslated region (UTR) in either the 3'-UTR or 5'-UTR of the target mRNAs. The IRP is known as RNA-binding proteins which interactions with IRE to control the translation which act as either a translational enhancer or a translational inhibitor depending on the position of the IRE in the mRNA. If IRP binds to IRE that located in the 5'-UTR of target mRNAs, it can inhibit the translation of target mRNAs including iron storage proteins (Ft-H and Ft-L) and iron export protein (FPN). While, the binding of IRP and IRE that located in the 3'-UTR of target mRNAs targets, it stabilizes the mRNA causing the increase in the expression of target mRNAs including iron import proteins (TfR1 and DMT1).

In iron deficiency condition, IRP can bind the IRE of target mRNAs. The translations of ferritin and FPN were inhibited causing the decrease of iron export and iron storage and the increase of free iron for cell usage, while the translations of TfR and DMT1 were increased leading to promote iron absorption into cells. Conversely, in iron repletion, IRP was binding by free iron causing a conformational change. It can cause the dissociation of IRP from IRE in the target mRNA. Therefore, the translations of the ferritin and FPN were promoted as well as TfR and DMT1 mRNA was destabilized (55, 56).

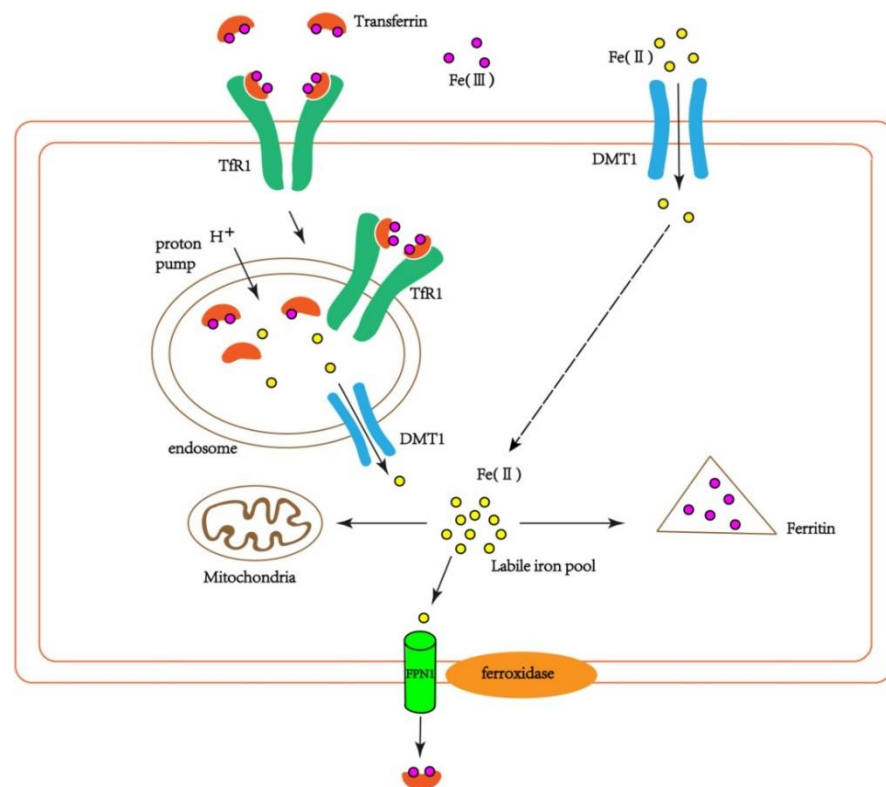


**Figure 3: The diagram of the iron transport mechanism**

The iron ( $\text{Fe}^{3+}$ ) transport into the cell by transferrin (Tf) binding to its receptor (TfR) mediated endocytosis to form endosomes in the cells. In the acidic endosome, due to the action of the proton pump, It affects Tf release  $\text{Fe}^{3+}$  and is reduced to  $\text{Fe}^{2+}$  which export from the endosome via divalent metal transporter1 (DMT1). The  $\text{Fe}^{2+}$  is utilized by the cell and is oxidized by ferritin and stored. Another part of  $\text{Fe}^{2+}$  is oxidized to ferric iron by the ferroxidase on the cell membrane and is exported by ferroportin (FPN) and recombined with extracellular Tf (57).

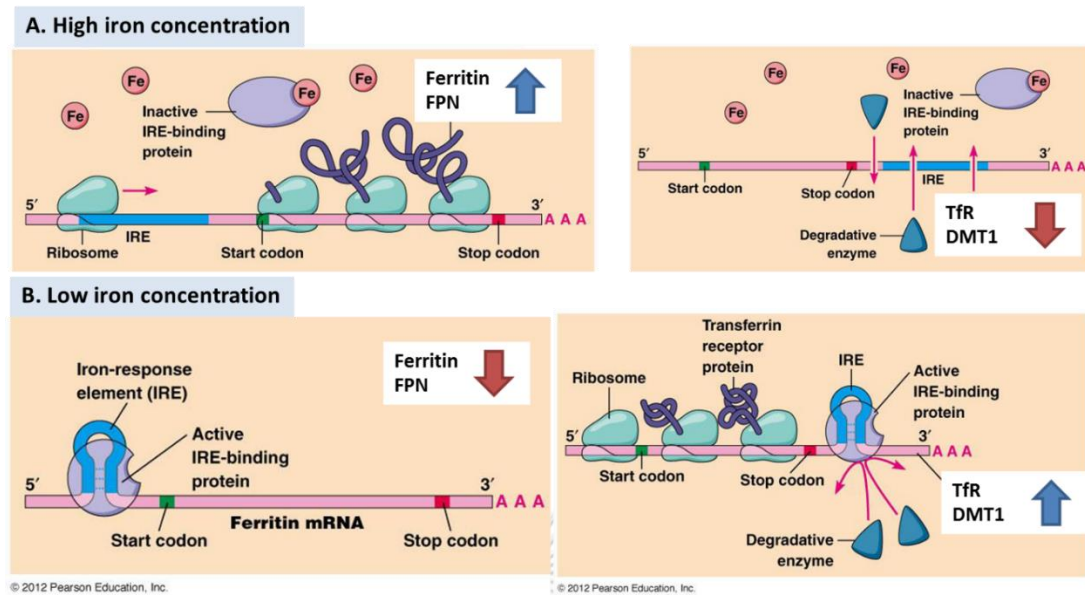


Figure 4: IRE-IRP pathway

The IRE-IRP pathway regulates iron homeostasis proteins depending on iron concentration. Ferritin mRNA and FPN mRNA contain IRE in 5'-UTR while Tfr mRNA and DMT1 mRNA contain IRE in 3'-UTR. When iron concentrations in cells are high (A), IRP is inactive form by binding with iron. Therefore, the translations of ferritin mRNA and FPN mRNA are processed. While Tfr mRNA and DMT1 mRNA are degraded and its syntheses are inhibited. For the low iron concentration (B), IRP can bind to IRE. So, ferritin and FPN translations are inhibited but the Tfr and DMT1 are synthesized (58).

## 2.6 Microglia

Microglia, constituting around 10% of all glial cells, they function as a resident immune cell in the central nervous system and originate from mesoderm. During embryonic development, microglia originate from early myeloid progenitors in the embryonic yolk sac and migrate to the neural tube and live for the life span of the organism by slowly dividing (59, 60). In physiological condition, microglia processes are a continuous motion for surveying the brain microenvironment and searching for brain damage to form the first line of defense. (1, 2) Upon brain infection or injury, microglia would change morphology reflect a highly activated state, cell bodies enlargement while cell processes are shortening. They also migrate to the injury site



and secrete cytokine mediators to maintain homeostasis and promote neuronal survival. Therefore, they are a crucial role in neuroprotection (1, 61).

### 2.6.1 Role of microglia

#### 1) Control synaptic density and synaptic plasticity

Microglia remove neurons that do not function during postnatal development and phagocyte dendritic spines to shape the neuronal synapses. The synaptic pruning was regulated by microglia via CX3CR1 (fractalkine receptor) interact with CX3CL1 (fractalkine ligand) expressed on the neuronal membrane (1). The previous study reported that the loss of CX3CR1-CX3CL1 interactions induced synaptic pruning delayed and reduced PSD95, a marker of excitatory postsynaptic density (62). The secretion of proinflammatory cytokines was impacting to synapse strength and plasticity. For instance, IL-1 $\beta$  produced by activated microglia can interfere with BDNF signaling which supports the dendritic spines formation for synaptic plasticity (63, 64).

#### 2) Prevent Excitotoxicity

The excessive release of excitatory neurotransmitters caused to excitotoxicity and induced neuronal damage and axonal swelling. Excitotoxicity also enhances neuronal damage releasing ATP that can activate the P2X7 receptor (ATP receptor) on microglia. Microglia prevent excitotoxicity by migrating to and covering around swollen axons that promote membrane repolarization (65).

#### 3) Protecting functions against injury

Microglia can act as a defense to against infectious pathogens, toxicity proteins such as amyloid beta (A $\beta$ ),  $\alpha$ -synuclein aggregation, and mutant or oxidized superoxide dismutase (SOD). Thus, microglia are express receptors that involved in these functions including Fc receptors, Toll-like receptors (TLRs), viral receptors, and antimicrobial peptides. Moreover, microglia are express phagocytic and endocytic receptors which enable to capture antigens. Therefore, microglia can function as

antigen-presenting cells (APCs) (1). Microglia initiated respond by produced cytokines and chemokines for recruitment of additional cells which clear injurious agents and maintain brain homeostasis. Neuroinflammation is different from peripheral inflammation which required leukocytes. The sustained neuroinflammation can induces neurotoxicity resulting to neurodegeneration.

#### 4) Cross talk of microglia and astrocytes

Astrocytes are glial cells in CNS that the most frequent cells around more than 50% of cells in CNS. Astrocyte morphology likes a star-shaped cell. Their processes contact with each other and form the network of coupled astrocyte. In addition, it covers the synaptic of neurons and also contacts the capillary vessel (2, 66). Astrocyte monitor the ion and neurotransmitters around synapses, they control the metabolic activity of neurons (67). Astrocytes direct many signals to microglia. In the model of laser injury, astrocytes activate rapid microglial response via releasing ATP (68). Astrocyte can release GABA and TGF- $\beta$  that inhibit microglial activation (69, 70). They also trigger the expression of NRF2 in microglia that induces the antioxidant molecule heme oxygenase 1 and controls the production of ROS (71).

##### 2.6.2 Microglia activation

In resting state, microglia are more branches and long processes that are continuous movement, protruding and retracting to cover long distances for survey large areas. This morphology calls ramified cells which can release neurotrophic factors such as insulin-like growth factor 1 (IGF1), brain-derived neurotrophic factor (BDNF), and nerve growth factor (NGF) (72). Their processes contact neurons astrocytes and blood vessels to regulate synaptic function (1). The ramified cells in resting state are regulated by CX3CL1-CX3CR1 interaction which contacts between neurons and microglia (73).

In brain injury, microglia are stimulated by inflammation or larger injury. Microglia immediately changed morphology from the ramified cells to amoeboid cells which expand the cell body and shorten cell process. This morphology reflects a highly

activated state correlated with phagocytosis and proinflammatory function (1). Activated microglia increase proliferation and phagocytose the damaged cells that are pathological and unnecessary of development. They release TNF- $\alpha$  that induces neuronal cell death and increase the expression of IL-1 $\beta$  (74, 75). Activated microglia also showed an increase in the expression of MHC-II that is the microglial activation marker (76). Moreover, they can secrete both anti-inflammatory cytokines and chemokine that show in table 1 (77). The overactivation of microglia may cause neurodegeneration. Therefore, the modulation of microglial activation was a current concepts to develop new strategies for neurodegenerative diseases.

**Table 1: The secretions from microglia**

Function	
Anti-inflammatory cytokines	<ul style="list-style-type: none"> <li>- Transforming growth factor beta (TGF- <math>\beta</math>)</li> </ul>
Neurotrophic factors	<ul style="list-style-type: none"> <li>- Brain-derived neurotrophic factor (BDNF)</li> <li>- Nerve growth factor (NGF)</li> <li>- Neurotrophin-3,4 (NT3,4)</li> </ul>
Chemokines	<ul style="list-style-type: none"> <li>- Monocyte chemoattractant protein 1 (MCP-1)</li> <li>- Macrophage inflammatory protein 1,2 (MIP-1,2)</li> <li>- Macrophage-derived chemokine/CCL22 (MDC)</li> </ul>
Neurotoxic	<ul style="list-style-type: none"> <li>- Nitric oxide (NO)</li> <li>- Superoxide (<math>O_2^{\cdot-}</math>)</li> <li>- Hydroxyl radical (<math>OH^{\cdot}</math>)</li> <li>- Hydrogen peroxide (<math>H_2O_2</math>)</li> </ul>
Proinflammatory cytokines	<ul style="list-style-type: none"> <li>- Interleukin-1<math>\beta</math> (IL-1<math>\beta</math>)</li> <li>- Interleukin-6 (IL-6)</li> <li>- Tumor necrosis factor alpha (TNF-<math>\alpha</math>)</li> </ul>

### 2.6.2.1 Stimulators of microglial activation

Based on previous reports in microglial cultures, microglia can be activated by several stimulators as following (78):

#### 1) Lipopolysaccharide (LPS)

LPS is the endotoxin-glycolipid of gram-negative bacterial outer cell wall. LPS can induce microglial activation which secreting various molecules including cytokines, chemokines and prostaglandin. Activating of inducible nitric oxide synthase (iNOS) and NO production in microglia were also stimulated by LPS. Moreover, the time of LPS stimulation have been interested. Previous report shown that the producing of cytokines are difference from the time of LPS stimulation. Tumor necrosis factor (TNF) is the first cytokine that releasing after 1 hour LPS stimulation, interleukin 1 $\beta$  (IL-1 $\beta$ ) was released within 3 hour and, finally IL-6.

#### 2) Interferon- $\gamma$ (IFN- $\gamma$ )

IFN- $\gamma$  has been reported to co-stimulated with LPS for inducing microglial activation (79). However, the IFN- $\gamma$  responses were not consistency in the microglia, the IFN- $\gamma$  is a common component in the cultured serum.

#### 3) Phorbol 12-Myristate 13-Acetate (PMA)

PMA is common stimulator for microglia by activating protein kinase C (PKC). PMA can promote proliferation in the low concentrations while high concentrations of PMA enhance superoxide (O<sub>2</sub><sup>-</sup>) productions (80).

#### 4) Amyloid $\beta$ (A $\beta$ ) protein

A $\beta$  is a senile plaques in the Alzheimer's brain. A $\beta$  peptides were used to stimulate microglia which have an important role in pathogenesis of Alzheimer's disease. A $\beta$  peptides enhance nitric oxide, IL-1 $\beta$  and TNF- $\alpha$  secretion from cultured microglia. In addition, the level of intracellular Ca<sup>2+</sup> was elevated in A $\beta$  stimulated microglia (81).

#### 5) Cytokines

Activated microglia produced several cytokines which also have an effect on microglia by themselves. Microglial proliferation was increased when exposed to IL-6

(82) while the level of intracellular  $\text{Ca}^{2+}$  in microglia was elevated after stimulated by  $\text{IL-1}\beta$ .

### 2.6.3 Cytotoxic of activated microglia

The stimuli that induce microglial activation are including lipopolysaccharide (LPS), interferon- $\gamma$  (IFN- $\gamma$ ) and amyloid- $\beta$ . These stimulators can induce microglia that produce multiple cytotoxic molecules such as superoxide anion, nitric oxide, and proinflammatory cytokines. It caused the neurotoxic effect (83). For example, ROS from activated microglia are toxicity particularly to myelin. Nitric oxide also induces DNA damage and causes neuronal cell death. Furthermore, the number of activated microglia were significantly increased in neurodegenerative disease and this condition terms as the microgliosis. Currently, microglial activation is important for neuronal survival, while the overactivation of microglia cause neurotoxicity that found in many neurodegenerative diseases (84).

### 2.6.4 Microglia and iron

Microglial iron pathways consist of the nontransferrin-bound iron uptake (NTBI) pathway and the canonical transferrin-bound iron (TBI) uptake pathway. For the NTBI uptake pathway, endogenous ferric reductase reduce ferric ion ( $\text{Fe}^{3+}$ ) to ferrous ion ( $\text{Fe}^{2+}$ ) at the cell surface and uptake into the cytoplasm by a divalent cation transporter 1 (DMT1). For the TBI uptake pathway, ferric binds to transferrin (Tf) and this binding form complex with transferrin receptor (TfR). Then, the complex becomes internalized by endocytosis. The acidic in the endosome promotes the complex of Tf and TfR release ferric ion. Ferric ion is reduced to ferrous ion and moved into the cytoplasm by DMT1 or other transporters (85, 86). Proinflammatory cytokine from activated microglia induce neuronal iron uptake (87) and also enhance microglia iron transport and metabolism (88, 89). The previous study found that microglial polarization induced by inflammation increased DMT1 expression. It implied that inflammation enhances iron accumulation in microglia by regulating DMT1 and FPN1 expression (90). In addition, LPS increased the expression of DMT1

and ferritin both transcription and translation protein in microglia cell line and also in primary mouse microglial cells. It demonstrated that microglia mostly increase uptake in the NTBI pathway for the response to proinflammation while uptake in the TBI pathway for the response to anti-inflammation (91). From these data, the model of the iron transport pathway in microglia is shown in figure 5.

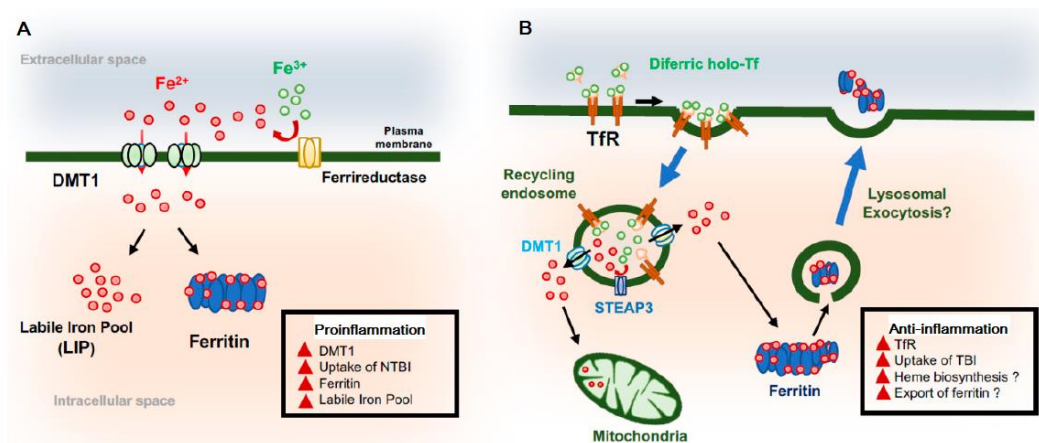


**Figure 5: Iron transport pathway in microglia**

(A) Pro-inflammatory increase divalent metal transporter 1 (DMT1) expression and increase uptake in the non-Tf-bound iron (NTBI) pathway. These are correlated with increased labile iron pool (LIP) and ferritin, iron storage protein. (B) Anti-inflammatory increase transferrin receptor (TfR) expression and increase uptake in Tf-bound iron (TBI). Modified from (48).

## 2.7 Microglia and Neurodegenerative diseases

Neurodegenerative diseases are affected to neuronal survival in the central nervous system (CNS), resulting in brain impairments. The common neurodegenerative diseases include Alzheimer disease (AD), Parkinson disease (PD), Huntington's disease (HD), and amyotrophic lateral sclerosis (ALS). The prevalence of neurodegenerative diseases is increasing in the elderly. Neurological disabilities were observed in these diseases such as memory impairment, and motor problems. Molecular studies have revealed that a typical feature of these diseases is specific protein accumulations as shown in table 2 (92).

**Table 2:** Protein aggregations in neurodegenerative diseases

Neurodegenerative diseases	Protein	Pathology feature
Alzheimer disease (AD)	A $\beta$ peptide Tau	Amyloid plaque Neurofibrillary tangle
Parkinson disease (PD)	$\alpha$ -synuclein	Lewy bodies
Huntington's disease (HD)	Huntingtin	Intranuclear inclusions Cytoplasmic aggregates
Amyotrophic lateral sclerosis (ALS)	Superoxide dismutase 1	Hyaline inclusions Axonal spheroids

In neurodegenerative diseases, microglia were observed with morphology as the activated phenotype might resulting from either protein aggregations or neuron degeneration. It has been demonstrated that in these diseases microglia become activation and expression the profiles of immune mediators such as TNF- $\alpha$ , IL-1 $\beta$ , ROS, and NO (93). AD and prion disease have extracellular aggregate protein which activated the microglia in the nearby (94). AD is the most common neurodegenerative diseases, presented the memory impairment. It is characterized by extracellular A $\beta$  plaque and intracellular neurofibrillary tangle of Tau protein. Normally, microglia can clearance A $\beta$  peptide but during A $\beta$  pathology in AD microglia failed to remove these resulting in A $\beta$  aggregates that also can activate microglia and cause damaged neuron. Moreover, these activated microglia produced inflammatory cytokines that further induced A $\beta$  deposition (1).

In some neurodegenerative diseases such as PD, ALS and HD have intracellular aggregate protein but these diseases still associated with microglial activation. PD is characterized by loss of dopamine neurons in the substantia nigra leading to motor impairment. It is accumulated misfolded  $\alpha$ -synuclein that activated microglia. The activated microglia and increase of inflammation was also found in the substantia nigra (94).

## CHAPTER III

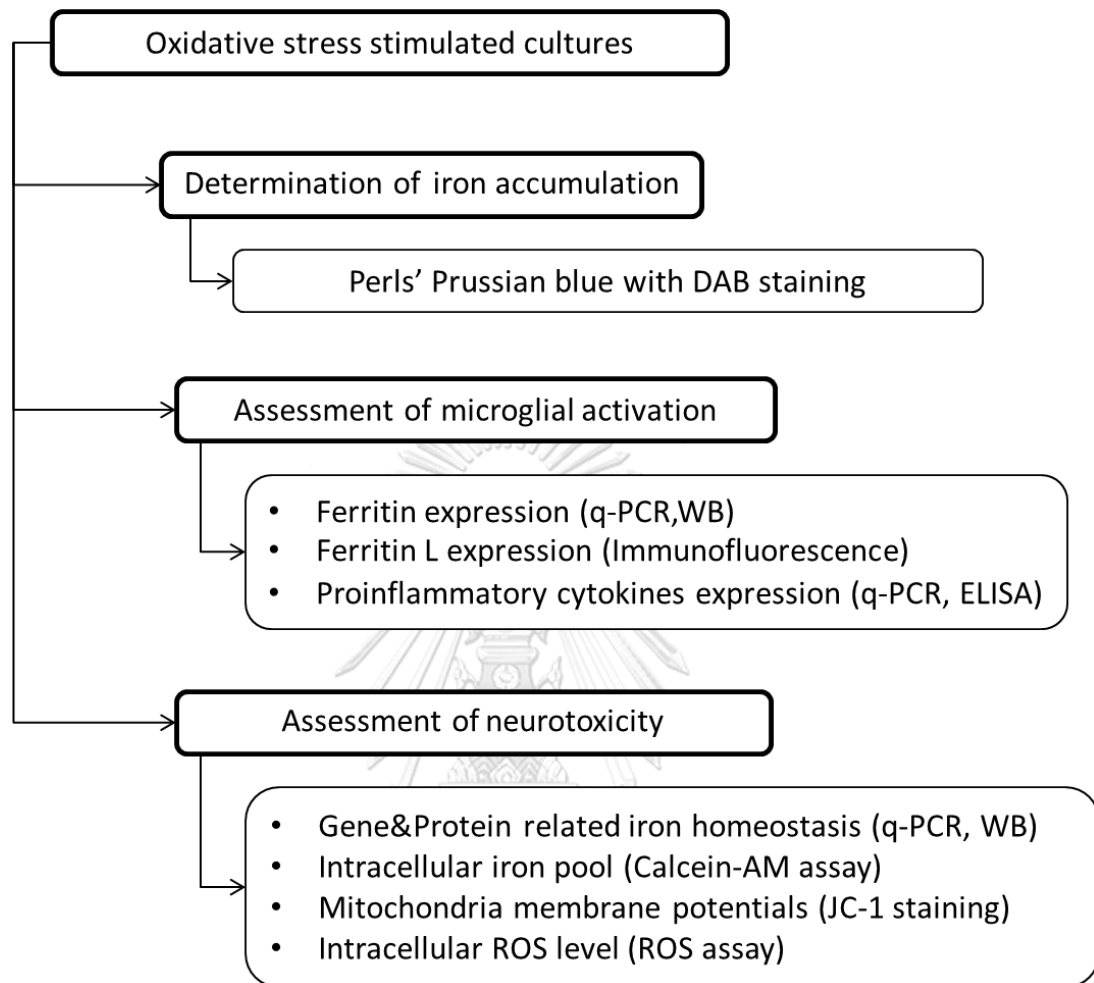
### MATERIALS AND METHODS

#### 3.1 Reagents

Dulbecco's modified Eagle's medium (DMEM) and cell culture supplements were from Hyclone (South Logan, UT, USA). Fetal bovine serum (FBS) was from Gibco (Thermo Scientific, USA). Trizol reagent, Revert-Aid First Strand cDNA Synthesis Kit, SYBR® Green PCR, protease inhibitor cocktails, BCA protein assay kit, Chemiluminescence reagent, and JC-1 dye were from Thermo Scientific (USA). Chloroform, Isopropanol, and 75% Ethanol were from Merck Millipore (USA). RIPA buffer, anti-ferritin heavy chain, anti- $\beta$ -Actin, and Calcein-AM were from Sigma-Aldrich (USA). Non-fat powdered milk (skim milk) was from Biobasic (Canada). Secondary antibody conjugated to horseradish peroxidase (HPR), anti-p16, anti-ferritin light chain, and anti-ferroportin1 were from Abcam (USA). Anti-DMT1 was from Santa Cruz. ELISA kits of TNF- $\alpha$ , IL-1 $\beta$ , and IL-6 were from ImmunoTools (Germany). ROS probe (CM-H2DCFDA) was from Molecular Probes. DAB+Substrate Chromogen was from Dako (Japan). AlexaFluor594 goat anti-rabbit secondary antibody and 4',6-Diamidino-2-Phenylindole, Dihydrochloride (DAPI) were from Invitrogen (USA).



### 3.2 Experimental design



### 3.3 Cell culture and treatment

Immortalized human microglial (HMC3) cells and human astrocytoma (1321N1) cells were kindly provided by Prof. James R Corner (The Pennsylvania State University, USA). Cells were cultured in Dulbecco's modified Eagle's medium (Hyclone, USA) supplemented with 5% fetal bovine serum (Thermo Scientific, USA), 1% penicillin/streptomycin (Hyclone, USA) and maintained at 37°C in a humidified 5% CO<sub>2</sub> incubator. The medium will be refreshed twice a week.

Microglia were directly stimulated oxidative stress by treating with/without 10uM of H<sub>2</sub>O<sub>2</sub> 4 hours per day for 4 days and indirectly stimulated oxidative stress via astrocyte conditioned medium (ACM) for 4 days. Astrocytes were treated with/without 10uM of H<sub>2</sub>O<sub>2</sub> 4 hours per day for 4 days. The astrocyte conditioned

medium was harvested from control astrocyte and H<sub>2</sub>O<sub>2</sub> stimulated astrocyte as the astrocyte conditioned medium (ACM) and the H<sub>2</sub>O<sub>2</sub> astrocyte conditioned medium (H<sub>2</sub>O<sub>2</sub>-ACM).

### **3.4 Cell viability by MTT assay**

To determine the concentrations of H<sub>2</sub>O<sub>2</sub> for stimulate microglia. The cell viability was measured by MTT assay. Cells were seeded into 96 well plate (2×10<sup>4</sup>cells/well) and were stimulated with H<sub>2</sub>O<sub>2</sub>. After that, cells were incubated with 0.5 mg/mL 4,5-dimethylthiazol-2-yl)-2,5-diphenyltetrazolium bromide (MTT) at 37°C for 2 hours. Then, formazan was dissolved in 75 µl of dimethyl sulfoxide (DMSO) and measured at 570 nm by the Synergy HT microplate reader. Cell viability was expressed as percentage (%) cell viability of control.

### **3.5 Ferric iron detection by Perls' Prussian blue staining with DAB enhancement**

The cellular ferric iron in microglia were evaluated by using Perls' Prussian blue staining with 3, 3'-diaminobenzidine (DAB) enhancement. Microglia were fixed with 10% Neutral buffered formalin for 10 min. Then, fixed cells were incubated in staining buffer that contains 20% of K<sub>4</sub>Fe (CN)<sub>6</sub> and 20% of HCl for 40 min. After washing with PBS, cells were enhanced the signaling by incubating in DAB+Substrate Chromogen (Dako, Japan) for 10 min. Finally, the cells were observed under the light microscope.

### **3.6 Intracellular iron detection by Calcein AM assay**

To determine changes in the labile iron pool (LIP) in microglia, fluorescent dye Calcein acetoxymethyl ester (Calcein-AM) (Sigma-Aldrich, USA) was used. Cells were incubated in 1 µM calcein AM for 30 min at 37°C in a humidified 5% CO<sub>2</sub> incubator and washed with PBS. Fluorescence was evaluated by using the Synergy HT microplate reader at excitation/emission wavelengths of 485/538 nm. The fluorescence intensity is quenched by iron binding to the receptor of Calcein. (95, 96) Thus, reduced fluorescence intensity reflects increasing labile iron pool in cells.

### 3.7 Western blotting

Western blotting was used to determine the expression of ferritin protein in both L subunit and H subunit which indicated to iron store in the cell. The proteins related to iron homeostasis were also evaluated including iron import and export proteins. Cells were lysed in RIPA buffer (Sigma-Aldrich, USA) and protease inhibitor cocktails (Thermo Scientific, USA), incubated on ice for 10 min. Protein concentration was determined by BCA protein assay kit (Thermo Scientific, USA) according to the manufacturer's protocol. Then, samples were separated by 10-12% sodium dodecyl sulfate-polyacrylamide gel electrophoresis (SDS-PAGE) and transferred to nitrocellulose membranes. The membranes were incubated with a primary antibody at 4 °C overnight after blocking with 1% skim milk in TBS-T. The primary antibodies included anti-ferritin heavy chain (1:1000, Sigma-Aldrich), anti-ferritin light chain (1:1000, Abcam, USA), anti-DMT1 (1:500, Santa Cruz), anti-ferroportin1 (1:1000, Sigma-Aldrich) and anti- $\beta$ -Actin (1:1000, Sigma-Aldrich) was used as an internal control. After washing, the membranes were incubated with a secondary antibody conjugated to horseradish peroxidase (HPR) (Abcam, USA) at room temperature for 2 hours and visualized by enhanced chemiluminescence reagent (Thermo Scientific, USA). The expression of protein was detected by densitometry measurement using the ChemiDoc™ Touch Imaging system.

### 3.8 Immunofluorescence assay

For immunofluorescence detection of ferritin light chain location, cells were fixed with 4% paraformaldehyde for 10 min. The fixed cells were permeabilized in 0.1% Triton-100-PBS for 10 min. Then, cells were incubated with an anti-ferritin light chain (1:500, Abcam, USA) as a primary antibody at 4 °C overnight after blocking with 2% normal goat serum. After washing, cells were incubated with an AlexaFluor594 goat anti-rabbit secondary antibody (1:1000, Invitrogen, USA) at room temperature for 2 hours. Nuclei were stained with 4',6-Diamidino-2-Phenylindole, Dihydrochloride (DAPI) (Invitrogen, USA). Images were captured with a digital camera under a Zeiss LSM800 confocal microscope equipped with Airyscan (Carl Zeiss, Germany).

### 3.9 RNA isolation and Quantitative Real-time Polymerase Chain Reaction (q-PCR)

To determine the expression of proinflammatory cytokine genes including IL-1 $\beta$ , IL-6 and TNF- $\alpha$  and the expression of iron homeostasis related genes including DMT1, FPN, Ft-H and Ft-L. Quantitative Real-time Polymerase Chain Reaction (q-PCR) was used. Total RNA was extracted from cells using Trizol reagent (Thermo Scientific, USA) according to the manufacturer's protocol. First, cell pellets were incubated in Trizol solution 1 ml and chloroform (Merck Millipore, USA) 200  $\mu$ l for 10 min and centrifuged 12,000 g for 15 min at 4°C. Then, supernatants were collected into the new tube. For RNA precipitation, Isopropanol (Merck Millipore, USA) was added 500  $\mu$ l incubated overnight at -20°C and centrifuged 12,000 g for 15 min at 4°C. After that, RNA pellets were washed by 75% Ethanol (Merck Millipore, USA) and dissolved in RNase free water. RNA samples were stored at -20 °C until use.

Revert-Aid First Strand cDNA Synthesis Kit (Thermo Scientific, USA) was used for cDNA synthesis. The volume of 1-2  $\mu$ g RNA from each sample was added into a reaction mixture containing 5X Reaction buffer, Oligo dT, Revert Aid, Ribolock and 10 mM dNTP. Then, the reactions were performed on the Applied Biosystems ProFlex PCR System (Thermo Scientific, USA). After that, cDNA template was used to determine the gene expression by Quantitative Real-Time PCR. The cDNA template was mixed with PCR reaction including Power SYBR® Green PCR (Thermo Scientific, USA) master mix, nuclease free water, forward primer, and reverse primer, the sequences are shown in table 3. The q-PCR analysis was performed on a StepOnePlus™ Real-Time PCR (Thermo Scientific, USA). The gene expression levels were calculated by the comparative cycle threshold ( $\Delta\Delta C_t$ ) after normalization to  $\beta$ -Actin as an endogenous control.

### 3.10 Enzyme-linked immunosorbent assay (ELISA)

The productions of proinflammatory cytokines (TNF- $\alpha$ , IL-1 $\beta$ , IL-6) from microglia were measured by using ELISA kit (ImmunoTools, Germany) according to the manufacturer's instructions. Briefly, the 96well-microplates were coated with

specific capture antibody overnight and subsequently incubated in blocking buffer (PBS + 2% BSA + 0.05% Tween20) for 1 hour and added standard cytokines and samples from supernatants for 2 hours. Then, incubation in biotinylated detector antibody and poly-HRP-Streptavidin using TMB as a substrate. The absorption at 450 nm was measured by using the Synergy HT microplate reader. Cytokine concentrations were calculated from standard curve generated with each cytokine.

**Table 3: Specific primers**

Gene	Primer sequences (5' → 3')
<b>Internal control</b>	
<b>βActin</b>	Forward primer: ACT CTT CCA GCC TTC CTT C Reverse primer: ATC TCC TTC TGC ATC CTG TC
<b>Proinflammatory cytokines</b>	
<b>IL-6</b>	Forward primer: GCC TTC GGT CCA GTT GCC TT Reverse primer: AGT GCC TCT TTG CTG CTT TCA C
<b>IL-1β</b>	Forward primer: CCT GTG GCC TTG GGC CTC AA Reverse primer: GGT GCT GAT GTA CCA GTT GGG
<b>TNF-α</b>	Forward primer: GGT CCT CTT CAA GGG CCA AG Reverse primer: CTC ACA GGG CAA TGA TCC CA
<b>Iron homeostasis</b>	
<b>DMT1 (+IRE)</b>	Forward primer: CCG GAA CAA TAA GCA GAA AGT T Reverse primer: GGA TGA TGG CAA TAG AGC GAG
<b>DMT1 (-IRE)</b>	Forward primer: TGG TTG CGG AGC TGA ATC AT Reverse primer: CCC AGG GGA CTG TGA AAG AG
<b>Ft-H</b>	Forward primer: GGT GCG CCA GAA CTA CC Reverse primer: CAT CAT CGC GGT CAA AGT AG
<b>Ft-L</b>	Forward primer: CCA GCA CCG TTT TTG TGG TT Reverse primer: TAG GAG GCC TGC AGG TAC AA

### 3.11 Intracellular Reactive Oxygen Species (ROS) assay

Cells were determined the intracellular ROS by using ROS-sensitive probe, 5-(and-6)-chloromethyl-2', 7'-dichlorodihydrofluorescein diacetate (CM-H2DCFDA) (Molecular Probes, Eugene). CM-H2DCFDA can enter into cells and is deacetylated by cellular esterases to DCFH. Then, ROS oxidize DCFH to the fluorescent 2',7'-dichlorofluorescein (DCF) as show in figure 6 (97). After induced cell with the conditioned medium, cells in 96-well plates were incubated with 10  $\mu\text{M}$  for 30 min. at 37°C in a humidified 5% CO<sub>2</sub> incubator and washed with PBS. Fluorescence intensity of DCF was measured by using Synergy HT microplate reader at excitation/emission wavelengths of 488/520 nm.

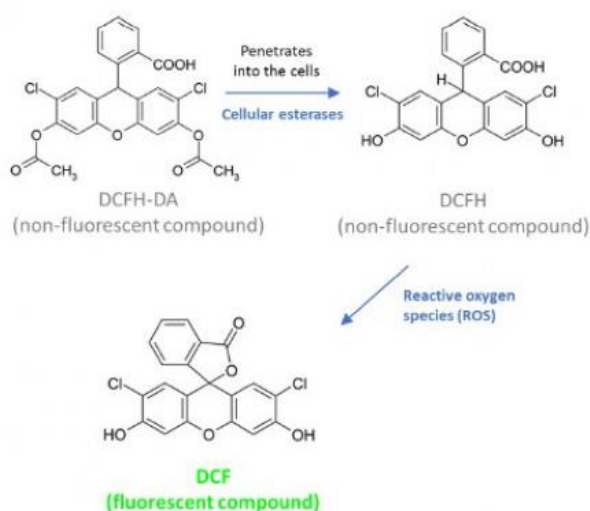


Figure 6: Mechanism of ROS assay

### 3.12 Mitochondrial Membrane Potential (MMP) $\Delta\psi_m$

Changes in the mitochondrial membrane potential  $\Delta\psi_m$  in HMC3 cells following treatments was examined using the fluorescence JC-1 dye (Invitrogen, USA) according to the manufacturer's instructions. Briefly, cells were incubated with the freshly prepared JC-1 solution (5  $\mu\text{M}$  in final concentration) for 20 min at 37°C in a humidified 5% CO<sub>2</sub> incubator and washed with PBS. After that, cells were observed under the fluorescence microscope. In healthy cells, JC-1 accumulates in mitochondria in a potential-dependent manner as J-aggregates with a red fluorescence emission maximum at 590 nm. In cells with mitochondria that lacks the

ability to maintain electrochemical potential across its membrane, JC-1 largely remains in the cytosol as monomers with a green fluorescence emission maximum at 535 nm. A reduction in the red to green fluorescence intensity ratio therefore indicates a decreased mitochondrial membrane potential  $\Delta\Psi_m$ .

### 3.13 Statistical analysis

Data were shown as the mean  $\pm$  standard error of mean (SEM). Statistical analyses were performed using SPSS 22.0 software (SPSS Inc., Chicago, IL, USA). One-way ANOVA followed by LSD's testing was used to compare groups. Statistical significance was defined by  $p < 0.05$ .



## CHAPTER IV

### RESULTS

#### 4.1 Iron accumulation was observed in microglia induced by H<sub>2</sub>O<sub>2</sub> ACM.

We initially studied the induction of oxidative stress in human microglial cell line (HMC3) induced by H<sub>2</sub>O<sub>2</sub>. To determine the concentration of H<sub>2</sub>O<sub>2</sub> which did not have cytotoxic effects, microglia were exposed to various concentrations of H<sub>2</sub>O<sub>2</sub> and cell viability was evaluated by MTT assay. As shown in figure 7, 15  $\mu$ M H<sub>2</sub>O<sub>2</sub> significantly affect the cell viability (\**p* =0.046). Thus, we select 10  $\mu$ M concentrations of H<sub>2</sub>O<sub>2</sub> which are the highest concentrations did not affect the cell viability. Then, microglia were exposed to 10 $\mu$ M of H<sub>2</sub>O<sub>2</sub> 4 hours per day for 4 days.

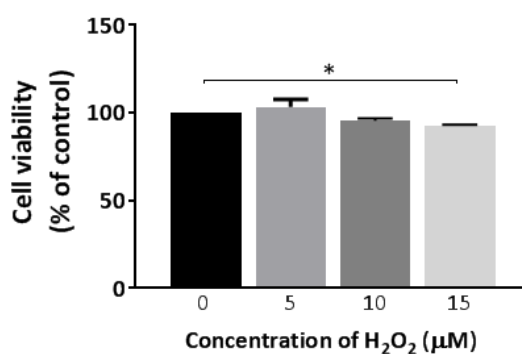


**Figure 7: Relative microglia cell viability determined by MTT assay.**

Microglia were exposed to 0 – 15  $\mu$ M of H<sub>2</sub>O<sub>2</sub> 4 hours per day for 4 days. After that, cell viability were measured by MTT assay. Results are expressed in graph bars as mean  $\pm$  SEM, n=3. Comparisons between groups were performed with one-way ANOVA with LSD's post hoc test, \**p* < 0.05.

In this study, we would like to establish the oxidative stress model that induced microglia accumulate iron. Therefore, we started by investigating the effect of oxidative stress on iron accumulation in microglia by observing the intracellular iron level in microglia. Perls' Prussian blue staining with DAB enhancement was used in this experiment to visualize the iron (ferric, Fe<sup>3+</sup>) deposits inside the cell which



shown in brown color. These results shown that iron positive cells were not observed in microglia that directly exposed to  $H_2O_2$  for 4 days and also similar in control microglia as shown in figure 8.

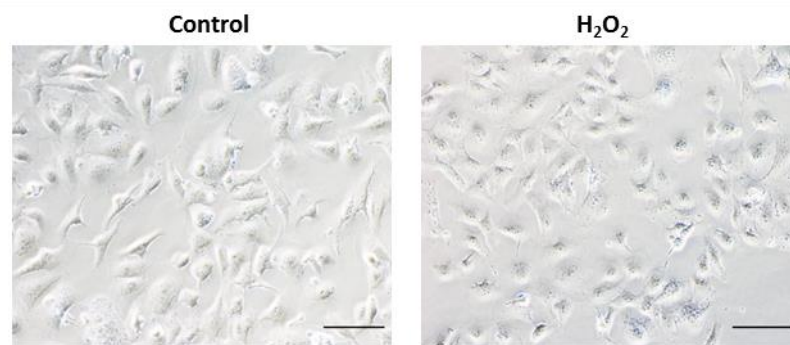


**Figure 8 Directly exposed oxidative stress did not induce iron accumulation in microglia.**

Shown the image of Perls' Prussian blue staining with DAB enhancement in microglia exposed to  $H_2O_2$  (10  $\mu M$ ) and without  $H_2O_2$  4 hours/day for 4 days. Scale bar equals 100  $\mu m$ .

According to these results, iron accumulation was not observed in microglia that exposed to directly oxidative stress. Therefore, we looked for another inducer for iron accumulation. Interestingly, the human brain tissue of Alzheimer's disease (AD) which involves  $\beta$ -amyloid ( $A\beta$ ) plaque deposition has surrounded by activated microglia and reactive astrocytes, while the role of these glial cells is still unclear (98). Moreover, these activated microglia were also observed the iron accumulation (99). Therefore, we hypothesized that astrocyte has some signaling associated with iron accumulation in activated microglia. Astrocytes as the most number of glial cells in the CNS have directed many signals to microglia and have controlled activation of microglia. Base on above stated reasons, we hypothesized that the secretions from oxidative stress-induced astrocytes have effects on microglial activation.

Therefore, we have studied the effect of indirect oxidative stress on microglia through the secretions from oxidative stress induced astrocytes. Astrocytes were exposed to  $H_2O_2$  similar to the induction in microglia and the medium at the last day were collected for cultured microglia for 4 days. The fresh medium was a control group of this experiment. This result shown that microglia indirectly exposed to  $H_2O_2$  via ACM were observed iron positive cells that highly increase in the  $H_2O_2$  ACM group than other groups as shown in figure 9.

As evidenced in this experiment, we next decided to study the effect of indirectly oxidative stress via ACM on microglia.

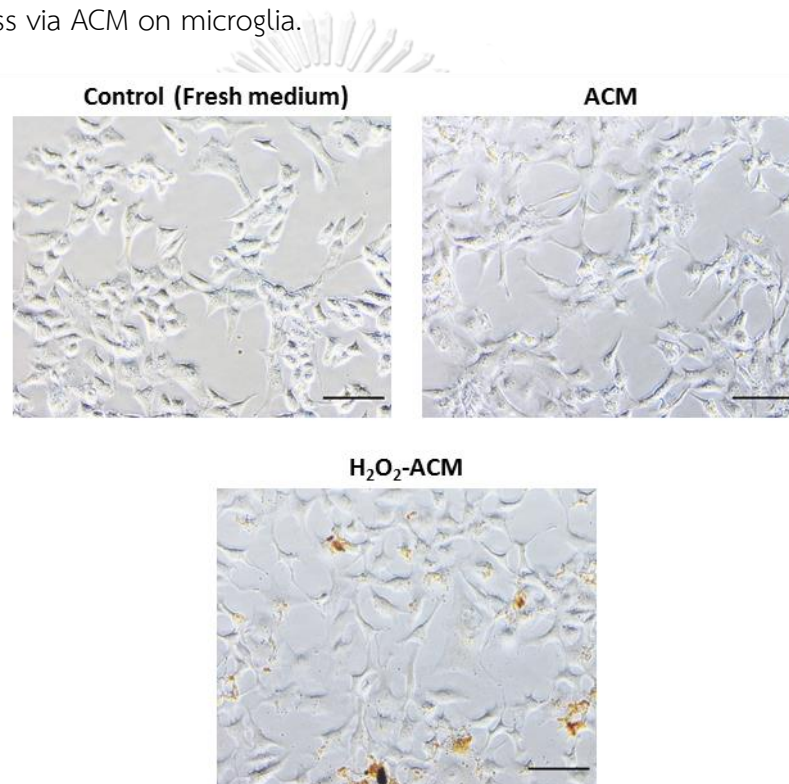


**Figure 9: Indirectly exposed oxidative stress via astrocyte conditioned medium induced iron accumulation in microglia.**

Shown the image of Perls' Prussian blue staining with DAB enhancement in microglia cultured in the fresh medium as a control, astrocyte conditioned medium (ACM) and  $H_2O_2$  (10  $\mu$ M) astrocyte conditioned medium ( $H_2O_2$ ACM) for 4 days. Brown color is iron positive cell. Scale bar equals 100  $\mu$ m.

#### 4.2 Microglia were activated by H<sub>2</sub>O<sub>2</sub> ACM.

Next, we determined the effect of oxidative stress on microglial activation which can detect by several markers including MHCII, Iba-I, and also ferritin (100, 101). Previous reports have demonstrated that microglia are expressed ferritin predominantly in amoeboid-reactive microglia (102). Therefore, the increase of ferritin expression can identify the increase of microglial activation. This experiment, the two subunits of ferritin including heavy chain subunit and light chain subunit were evaluated as shown in figure 10A-F. After cultured microglia in H<sub>2</sub>O<sub>2</sub> ACM for 4 days, the mRNA expression of ferritin heavy chain in H<sub>2</sub>O<sub>2</sub> ACM group was no significant difference from control group ( $p = 0.986$ , Fig.10A) while ACM group was significantly increased in the mRNA expression of ferritin heavy chain when compared to control group (\*\* $p < 0.001$ , Fig.10A) and also H<sub>2</sub>O<sub>2</sub> ACM group (\*\* $p < 0.001$ , Fig.10A). Similarly, the protein expression of ferritin heavy chain in ACM group was dramatically elevated when compared to the control group and H<sub>2</sub>O<sub>2</sub> ACM group (\*\* $p < 0.001$  and \* $p = 0.001$ , respectively; Fig.10B-C). The H<sub>2</sub>O<sub>2</sub> ACM group was higher in the protein expression of ferritin heavy chain than control group (\* $p = 0.002$ , Fig.10B-C).

The expressions of ferritin light chain both transcriptional level and the translational level were significantly higher in H<sub>2</sub>O<sub>2</sub> ACM group than in control group and ACM group. The mRNA expression of the ferritin light chain was significantly higher in H<sub>2</sub>O<sub>2</sub> ACM group than in control group and ACM group (\*\* $p < 0.001$  and \* $p = 0.012$ , respectively; Fig.10D). The ferritin light chain protein expression was also significantly increased in H<sub>2</sub>O<sub>2</sub> ACM group when compared to control group and ACM group (\* $p = 0.04$  and \* $p = 0.022$ , respectively; Fig.10E-F). There were no statistically significant difference in the ferritin light chain mRNA expression or the protein expression between ACM group and control group ( $p = 0.159$  and  $p = 0.668$ , respectively; Fig.10D-F).

These data indicated that microglia exposing to indirectly oxidative stress via ACM increased microglial activation which indicating by elevating the ferritin expression, especially in light chain subunit. Therefore, and based on these results, we

additionally observed the ferritin light chain expression by using immunofluorescence staining.

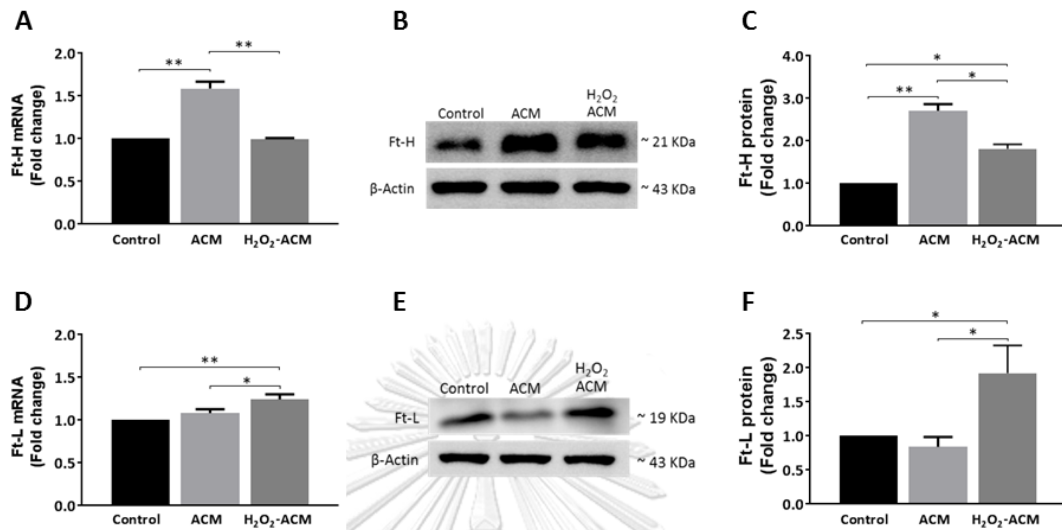
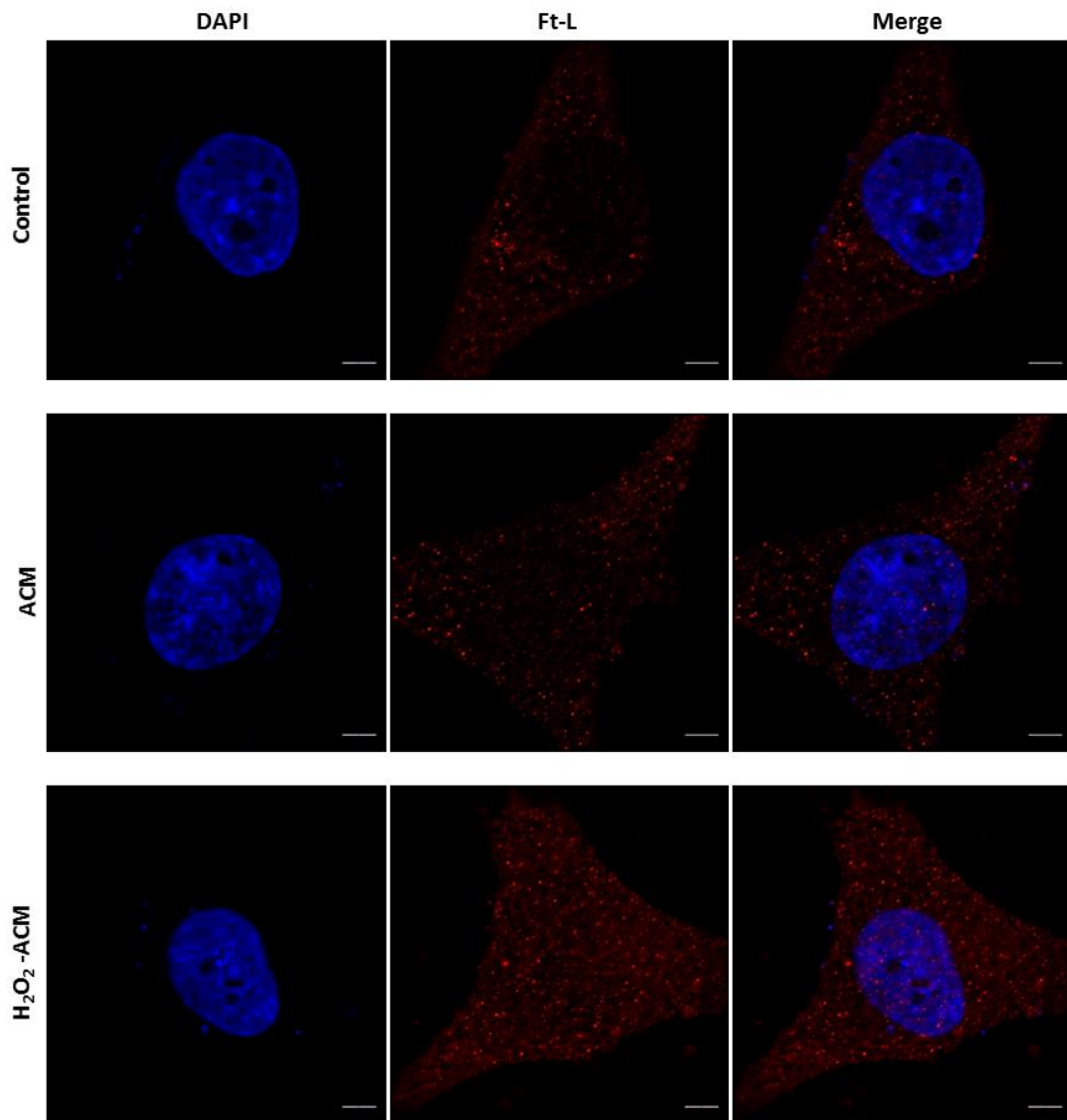


**Figure 10: Indirectly exposed oxidative stress via astrocyte conditioned medium induced microglia activation.**

Microglia cultured in the fresh medium as a control, astrocyte conditioned medium (ACM) and H<sub>2</sub>O<sub>2</sub> (10 μM) astrocyte conditioned medium (H<sub>2</sub>O<sub>2</sub>ACM) for 4 days. **(A-C)** Ferritin heavy chain/Ft-H expression was determined by q-PCR for mRNA level and western blot for protein level. The quantitative densitometric analysis is represented in graph bars as mean ± SEM, n=3. **(D-F)** Ferritin light chain/Ft-L expression was determined by q-PCR for mRNA level and western blot for protein level. The quantitative densitometric analysis is represented in graph bars as mean ± SEM, n=3. Comparisons between groups were performed with one-way ANOVA with LSD's post hoc test, \* p < 0.05, \*\*p < 0.001.

The ferritin L subunit facilitates mineralization and stabilizes the ferritin complex structure which associated with iron storage in a long-term (49, 50). Previous study reported that microglia are mostly to express the ferritin L indicating that these cells provide iron storage (52, 53). As shown in figure 11, the ferritin L protein was found in the cytoplasm of microglia every conditions and more increased in the H<sub>2</sub>O<sub>2</sub> ACM group.



SRINAKHARIN UNIVERSITY

Figure 11: Ferritin light chain protein was increased in the H<sub>2</sub>O<sub>2</sub> astrocyte conditioned medium group.

Representative confocal images of the immunofluorescence staining (Ferritin light chain: red, DAPI: blue) in microglia cultured in the fresh medium as a control, astrocyte conditioned medium (ACM) and H<sub>2</sub>O<sub>2</sub> (10 μM) astrocyte conditioned medium (H<sub>2</sub>O<sub>2</sub>ACM) for 4 days. Scale bar equals 5 μm.

Moreover, activated microglia can secrete multiple cytotoxic molecules such as superoxide anion, nitric oxide, and also proinflammatory cytokines (83). Therefore, the expressions of proinflammatory cytokines were evaluated in this study to confirm the activation of microglial activation after exposed to oxidative stress. We determined both mRNA expression and protein secretion of IL-1 $\beta$ , IL-6, and TNF- $\alpha$ . As shown in figure 12, microglia in H<sub>2</sub>O<sub>2</sub> ACM group were higher level in IL-1 $\beta$ , IL-6, and TNF- $\alpha$  both mRNA expression and protein secretion than control group and ACM group.

The mRNA expression of IL-1 $\beta$  in H<sub>2</sub>O<sub>2</sub> ACM group on the 4<sup>th</sup> day was significantly higher than the control group and ACM group (\**p* = 0.004 and \**p* = 0.010, respectively; Fig.12A). On the 3<sup>rd</sup> day, the IL-1 $\beta$  mRNA expression was higher in the H<sub>2</sub>O<sub>2</sub> ACM group than the control group (\**p* = 0.029; Fig.12A) while on the 2<sup>nd</sup> day the IL-1 $\beta$  mRNA expression was no significant difference among three groups.

The IL-6 mRNA expression on the 4<sup>th</sup> day was higher in the H<sub>2</sub>O<sub>2</sub> ACM group than the control group and ACM group (\*\**p* < 0.001 and \**p* = 0.001, respectively; Fig.12B) and also on the 3<sup>rd</sup> day (\**p* = 0.001 and \**p* = 0.001, respectively; Fig.12B). While on the 2<sup>nd</sup> day the IL-6 mRNA expression was no significant difference among three groups.

The mRNA expression of TNF- $\alpha$  on the 4<sup>th</sup> day statistically increased only in H<sub>2</sub>O<sub>2</sub> ACM group when compared to the control group and ACM group (\*\**p* < 0.001 and \*\**p* < 0.001, respectively; Fig.12C). On the 3<sup>rd</sup> day, the mRNA expression of TNF- $\alpha$  moderately elevated in ACM group as well as in H<sub>2</sub>O<sub>2</sub> ACM group when compared to control group (\*\**p* < 0.001 and \*\**p* < 0.001, respectively; Fig.12C). The mRNA expression of TNF- $\alpha$  elevated in H<sub>2</sub>O<sub>2</sub> ACM group when compared to ACM group (\**p* = 0.047; Fig.12C). Notably, TNF- $\alpha$  mRNA expression on the 2<sup>nd</sup> day was only significant increased in H<sub>2</sub>O<sub>2</sub> ACM group than in control group (\**p* = 0.007; Fig.12C) while IL-1 $\beta$  and IL-6 mRNA expression was no significant difference among three groups (Fig.12A-B). All of these cytokines in H<sub>2</sub>O<sub>2</sub> ACM group were more continuously increased on the 3<sup>rd</sup> and 4<sup>th</sup> days.

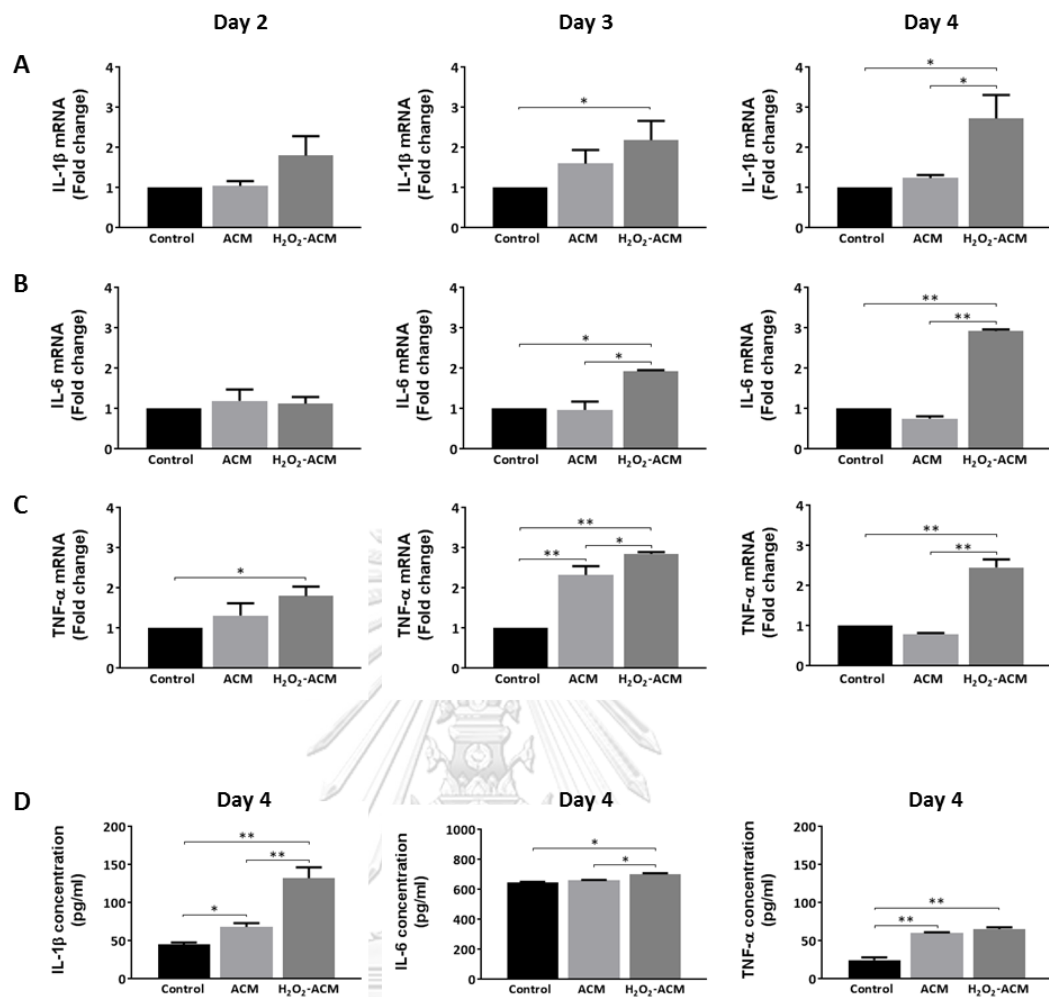


Figure 12: Indirectly exposed oxidative stress via astrocyte conditioned medium microglia induced the expressions of proinflammatory cytokines.

Microglia were cultured in the fresh medium as a control, astrocyte conditioned medium (ACM) and H<sub>2</sub>O<sub>2</sub> astrocyte conditioned medium (H<sub>2</sub>O<sub>2</sub>ACM) for 4 days. The expression of IL-1 $\beta$  (A), IL-6 (B) and TNF- $\alpha$  (C) were determined by q-PCR. (D) The secretion of IL-1 $\beta$ , IL-6, and TNF- $\alpha$  was evaluated by ELISA. Results are expressed in graph bars as mean  $\pm$  SEM, n=3. Comparisons between groups were performed with one-way ANOVA with LSD's post hoc test, \*p < 0.05 and \*\*p < 0.001.

In addition, IL-1 $\beta$ , IL-6, and TNF- $\alpha$  secretion on the last day were analyzed by using ELIZA assay as shown in figure 12D. Similarly, these cytokines were more produced by microglia in H<sub>2</sub>O<sub>2</sub> ACM group than the other groups. Microglia in H<sub>2</sub>O<sub>2</sub> ACM group shown an increased production of IL-1 $\beta$  when compared to the control group and ACM group (\*\* $p$  < 0.001 and \*\* $p$  < 0.001, respectively; Fig.12D). Microglia in ACM group also shown an increased production of IL-1 $\beta$  when compared to the control group (\* $p$  =0.040; Fig.12D). According to the production of IL-6, there was higher in H<sub>2</sub>O<sub>2</sub> ACM group than in the control group and ACM group (\* $p$  =0.001 and \* $p$  =0.011, respectively; Fig.12D) and there was no statistically significant difference between the control group and ACM group ( $p$  =0.283; Fig.12D). Indeed, the production of TNF- $\alpha$  in H<sub>2</sub>O<sub>2</sub> ACM group was significantly higher than the control group (\*\* $p$  < 0.001; Fig.12D) while there was no significant difference between H<sub>2</sub>O<sub>2</sub> ACM group and ACM group ( $p$  =0.174; Fig.12D). Microglia in ACM group also significantly increased the production of TNF- $\alpha$  when compared to the control group (\*\* $p$  < 0.001; Fig.12D).

Altogether these data suggest that H<sub>2</sub>O<sub>2</sub> ACM induced microglial activation which more express the proinflammatory cytokines.

#### 4.3 Iron homeostasis in microglia was altered by H<sub>2</sub>O<sub>2</sub> ACM.

According to increasing in iron positive cell and ferritin expression, there was indicated that H<sub>2</sub>O<sub>2</sub> ACM induced microglial activation with iron accumulation and affected to iron storage proteins. The activated microglia with iron accumulation have be demonstrated that vulnerable to neuronal survival by producing free radical (3). To explore the mechanism of iron accumulation in activated microglia, the level of intracellular iron, mRNA expression and protein levels of cellular iron homeostasis were assessed. The Calcein-AM assay was used to measure the level of intracellular iron, the decrease of Calcein-AM fluorescent intensity implied to increase the iron levels. As shown in figure 13A, there was no significant difference among the three groups.



We investigated the relative mRNA expression and protein levels of cellular iron homeostasis including iron export and iron import. This finding shown that after cultured microglia in H<sub>2</sub>O<sub>2</sub> ACM for 4 days, microglia were reduced in iron export and elevated in iron import. We determined the mRNA expression of divalent metal transporter 1 (DMT1), involved in iron import from endosomes to cytoplasm, both DMT1 with an iron-responsive element (IRE) in the 3' untranslated region (DMT1+IRE) regulate iron homeostasis via response to dietary iron status and DMT1 non IRE which lacks the IRE domain (DMT1-IRE) (103).

The mRNA expression of DMT1+IRE was significantly higher in H<sub>2</sub>O<sub>2</sub> ACM group than in control group (\**p* =0.009; Fig.13B) and the DMT1+IRE mRNA expression in ACM group was also significantly higher than the control group (\**p* =0.034; Fig.13B). There was no significant difference in the DMT1+IRE mRNA expression between H<sub>2</sub>O<sub>2</sub> ACM group and ACM group (*p* =0.524; Fig.13B).

According to the mRNA expression of DMT1-IRE, there was significantly higher in H<sub>2</sub>O<sub>2</sub> ACM group than in the control group and ACM group (\*\**p* < 0.001 and \**p* =0.004, respectively; Fig.13C). Microglia in ACM group also shown an increased expression of DMT1-IRE when compared to the control group (\**p* =0.005; Fig.13C).

Indeed we confirmed by evaluated the DMT1 protein expression which is a total form as shown in figure 13E. The result shown that microglia in H<sub>2</sub>O<sub>2</sub> ACM group sharply elevated in DMT1 protein expression when compared to the control group and ACM group (\**p* = 0.009 and \**p* = 0.040, respectively; Fig.13E). We did not observe differences in DMT1 protein expression between ACM group and control group (*p* =0.871; Fig.13E).

Conversely, microglia in H<sub>2</sub>O<sub>2</sub> ACM group was significantly lower in the ferroportin (FPN) protein expression, function to efflux iron from the cell, than the control group and ACM group (\**p* = 0.026 and \**p* = 0.032, respectively; Fig.13D). There was no significant difference in FPN protein expression between ACM group and the control group (*p* =0.871; Fig.13D).

These results suggested that the iron accumulation in microglia exposed by the indirectly oxidative stress was associated with an alteration of iron homeostasis which increased the iron import protein and decreased the iron export protein.

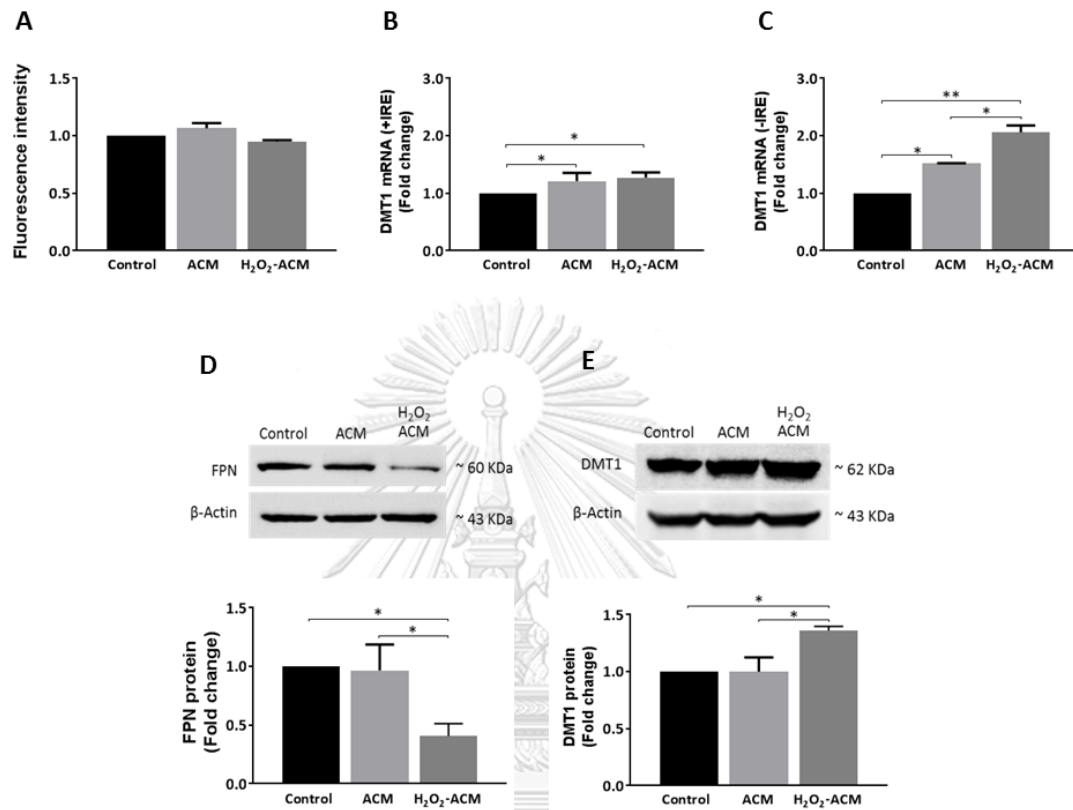


**Figure 13: Indirectly exposed oxidative stress via astrocyte conditioned medium altered iron homeostasis in microglia.**

Microglia were cultured in the fresh medium as a control, astrocyte conditioned medium (ACM) and H<sub>2</sub>O<sub>2</sub> astrocyte conditioned medium (H<sub>2</sub>O<sub>2</sub>-ACM) for 4 days. **(A)** Calcein-AM fluorescence intensity in microglia represented in graph bars as mean ± SEM, n=3. Reduced fluorescence intensity reflects increasing the level of intracellular iron. **(B)** The expression of divalent metal transporter 1 with iron-responsive element (IRE) (+IRE) and **(C)** without iron-responsive element (-IRE) was determined by q-PCR. **(D)** The protein expression of ferroportin/FPN and **(E)** DMT1 was evaluated by western blot. The quantitative densitometric analysis is represented in graph bars as mean ± SEM, n=3. Comparisons between groups were performed with one-way ANOVA with LSD's post hoc test, \**p* < 0.05 and \*\**p* < 0.001.

#### 4.4 The increasing of ROS and mitochondrial dysfunction was shown in microglia induced by H<sub>2</sub>O<sub>2</sub> ACM.

Mitochondria are critical function in cellular energy and essential for cellular functions including cellular differentiation, regulation growth cycle, and cell death. The loss of mitochondrial membrane potential ( $\Delta\Psi_m$ ) is indicated the unhealthy cell and affects to the ROS levels resulting to oxidative damage (104). Thus, we investigated the ROS levels by using ROS-sensitive probe (CM-H<sub>2</sub>DCFDA) and mitochondrial membrane potential (MMP) by using JC-1 probe.

The result shown that the H<sub>2</sub>O<sub>2</sub> ACM can cause intracellular ROS levels increased and MMP decreased in microglia (Fig.14). The intracellular ROS levels in H<sub>2</sub>O<sub>2</sub> ACM group were higher especially on the 2<sup>nd</sup> day than the control group and ACM group (\*\**p* < 0.001 and \*\**p* < 0.001, respectively; Fig.14A). Microglia in ACM group were significantly increased in the intracellular ROS levels when compared to the control group (\**p* = 0.015; Fig.14A). The result of the 3<sup>rd</sup> day shown that the intracellular ROS moderately elevated in H<sub>2</sub>O<sub>2</sub> ACM group when compared to the control group and ACM group (\**p* = 0.001 and \**p* = 0.003, respectively; Fig.14A) and there was no significant difference in the intracellular ROS levels between ACM group and the control group (*p* = 0.583; Fig.14A). Moreover, on the last day, microglia in H<sub>2</sub>O<sub>2</sub>-ACM group and ACM group slightly elevated in the intracellular ROS levels when compared to the control group (\**p* = 0.001 and \**p* = 0.014, respectively; Fig.14A).

According to JC-1 fluorescence images (Fig.14B), red fluorescence due to J-aggregate formation indicates high MMP, whereas green fluorescence of the JC-1 monomers indicates depolarized MMP. This result found that microglia cultured in H<sub>2</sub>O<sub>2</sub> ACM were observed more green fluorescent than red fluorescent conversely to microglia in other groups. It is implied that the MMP of microglia cultured in H<sub>2</sub>O<sub>2</sub> ACM was decreased when compared to other groups.

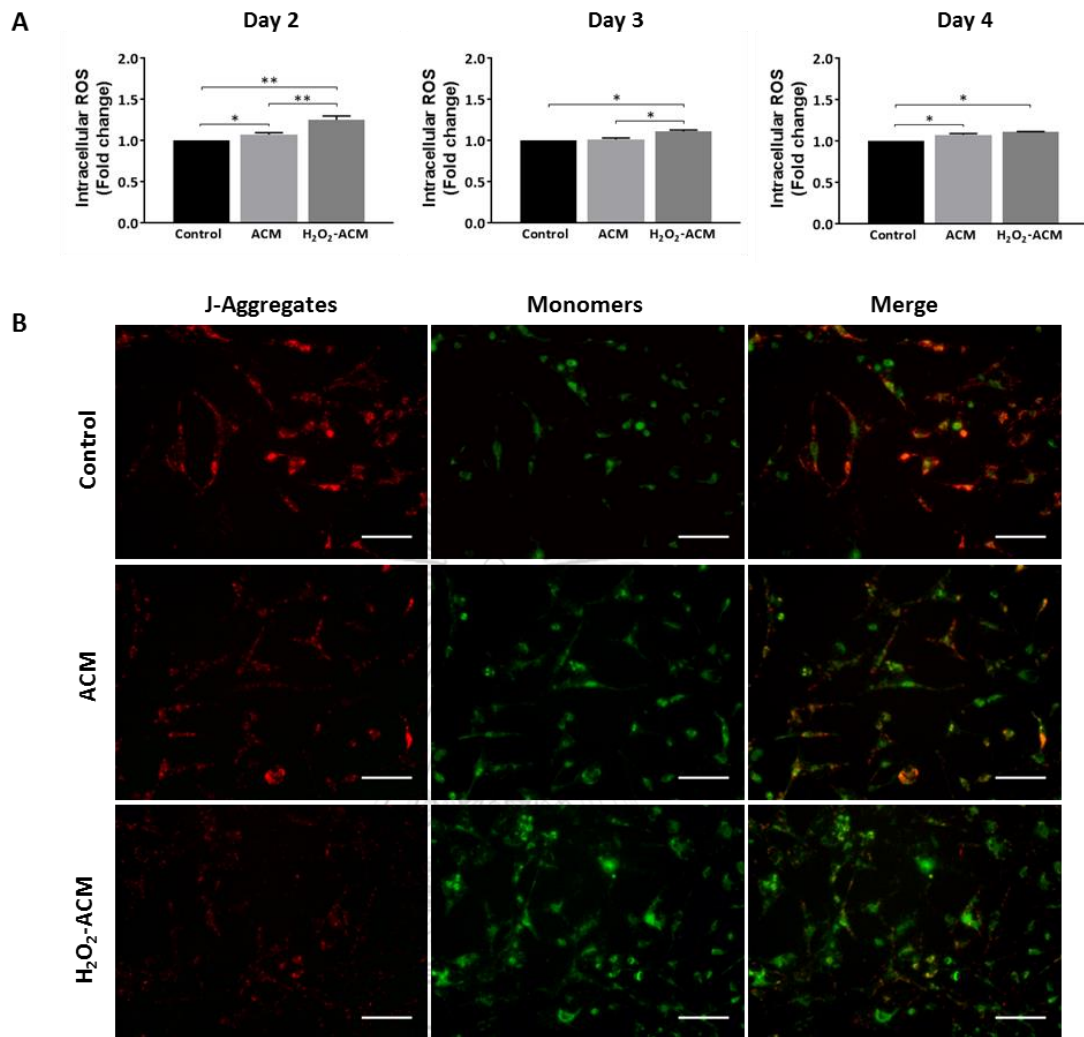


Figure 14: Indirectly exposed oxidative stress via astrocyte conditioned medium increased ROS levels and decreased mitochondria membrane potential in microglia.

Microglia were cultured in the fresh medium as a control, astrocyte conditioned medium (ACM) and H<sub>2</sub>O<sub>2</sub> astrocyte conditioned medium (H<sub>2</sub>O<sub>2</sub>ACM) for 4 days. **(A)** Intracellular ROS levels were determined by ROS-sensitive probe (CM-H2DCFDA). Results are expressed in graph bars as mean  $\pm$  SEM, n=3. Comparisons between groups were performed with one-way ANOVA with LSD's post hoc test, \*p < 0.05 and \*\*p < 0.001. **(B)** Mitochondria membrane potential was determined by JC-1 probe that representative the JC-1 fluorescence images (Aggregates: Red, Monomer: Green). Scale bar equals 100  $\mu$ m.

## CHAPTER V

### DISCUSSION AND CONCLUSION

The present study was designed to investigate the effect of oxidative stress to iron accumulation and microglial activation. We determined the iron accumulation, the markers of microglial activation and also observed the iron homeostasis proteins alteration. Our data indicated that the directly expose oxidative stress to microglia did not induce iron deposition while the indirectly oxidative stress via H<sub>2</sub>O<sub>2</sub> ACM induced iron deposition and microglial activation. These microglia evidenced the markers of activated microglia as increased ferritin expression, elevated proinflammatory cytokines, increased ROS level, and decreased mitochondria membrane potential. Moreover, these microglia were found iron accumulation thought changed in iron homeostasis proteins which increased DMT1-iron import protein and decreased FPN-iron export protein.

The present study shown that H<sub>2</sub>O<sub>2</sub> ACM induce microglial activation, while directly oxidative stress did not induce microglial activation. It is possible that the stress-astrocyte can produce many complex signaling not only oxidative stress mediators but also inflammatory factors. Generally, microglia can activated by several mediators including endotoxin, mitogens, and also cytokines (105) which may found in H<sub>2</sub>O<sub>2</sub> ACM. In line with previous reports, H<sub>2</sub>O<sub>2</sub> can stimulate astrocyte secret TNF- $\alpha$  (106) which have been reported that induced microglial activation (107, 108). Furthermore, astrocytes can regulate microglial activation and functions through numerous astrocyte-secretions, such as cytokines, chemokines, Ca<sup>2+</sup>, complement proteins, and other inflammatory mediators (109). Previous study have been reported that hippocampal astrocytes enhanced microglial activation by deriving Lipocalin-2 (LCN2) which interact with their receptor on microglia resulting hippocampal damage and cognitive impairment in the rodent models of vascular dementia (110).

This study found significantly higher levels of proinflammatory cytokines in activated microglia. This is in line with a previous study indicating that LPS induced microglial activation that observed by the elevation of MHC-II and OX42 expression and also found the release of pro-inflammatory cytokines such as IL-1 $\beta$ , IL-6, and TNF- $\alpha$  causing neuroinflammation which developed to oligodendrocyte death and demyelination. Interestingly, TNF- $\alpha$  blocking can prevent oligodendrocyte death and myelin damage (111). Activated microglia produced cytotoxic proteins including chemokines, proteinases, and cytokines such as TNF- $\alpha$ , IL-6, monocyte chemoattractant protein-1 (MCP-1) (83). Their productions are typically intended to damage the CNS and also be toxic to neurons and other glial cells. Nowadays, microglial activation and their production of proinflammatory cytokines were targeted in the treatment of neurodegenerative disease. Therefore, H<sub>2</sub>O<sub>2</sub> ACM group increased proinflammatory cytokines level in microglial activation also can imply the increase of cytotoxicity to the brain.

Interestingly, we noted that IL-6 production of microglia in the control group was high level, which is in agreement with previous studies that shown the baseline of IL-6 production by human microglia cell line are high levels ranged between 20 and 950 pg/ml in serum free medium after 24-h incubation (112-114). Moreover, the result shown that H<sub>2</sub>O<sub>2</sub> ACM increased the secretion of TNF- $\alpha$  at the 2<sup>nd</sup> while other cytokines did not increase. This is in line with a previous study indicating that the producing of cytokines are different with the time of LPS stimulation. TNF- $\alpha$  is the first cytokine that releasing after LPS stimulation, then IL-1 $\beta$  was released and finally IL-6 (78). For the innate immune response, TNF- $\alpha$  is the first initiator response and it promoted TNF- $\alpha$  production and also IL-1 production as the autocrine action. Then, IL-1 induced neighboring cells as a paracrine action resulting produced IL-6 (115). These indicated that the response of microglial activation is different in time-dependent.

Ferritin is the main iron storage protein. It consists of L and H subunits. Ferritin H (Ft-H) subunit functions as a ferroxidase, catalyzes  $\text{Fe}^{2+}$  to  $\text{Fe}^{3+}$ , while ferritin L (Ft-L) subunit facilitates mineralization and stabilizes the ferritin complex structure (49, 50). Interestingly, our data found that microglial activation increased ferritin expression, particularly in the Ft-L subunit. This could partially be explained by previous reports that the Ft-L subunit was more observed in microglia than the Ft-H subunit (116, 117). Moreover, the increases of Ft-L may cause to promote long term iron storage (118). We noted that microglia in  $\text{H}_2\text{O}_2$  ACM group increased ferric iron measuring by Perls' Prussian blue staining with DAB enhancement while did not change in the intracellular iron measuring by Calcein-AM assay. It is in accordance with the increase of ferritin expression that stores iron in the ferric form may cause an increase in only ferric iron not the intracellular iron.

The altered iron homeostasis observed in microglial activation is in line with recent data showing that treatment of microglia *in vitro* with  $\text{TNF-}\alpha$  and  $\text{TGF-}\beta 1$  increased the expression of the iron importer (DMT1) and decreased the expression of the iron exporter (FPN). They suggested that these cytokines which expressed in CNS inflammation of neurodegenerative diseases can possibly be profound effects on iron homeostasis in microglia (119).

DMT1 mediates the transport of ferrous iron from the plasma membrane or endosomes to the cytoplasm. DMT1 +IRE is regulated by intracellular iron levels via the IRE/IRP system while DMT1 -IRE is regulated by iron-independent mechanisms (120, 121). Therefore, we also determined the expression of DMT1 +IRE and DMT1 -IRE and noted that the elevation of DMT1 gene expression in microglial activation was significantly higher in DMT1-IRE than DMT1 +IRE. This could be implied that the iron homeostasis in microglial activation did not regulate by iron status. It may be a pathological situation.

The mitochondrial membrane potential (MMP) is a critical component in the cellular energy process which generated by proton pumps. The loss of MMP is indicated the mitochondria dysfunction in unhealthy cell and affect to the ROS levels, leading to pathological consequences. Mitochondria dysfunction occurs in

most neurodegenerative diseases, including Alzheimer's (AD), Parkinson's diseases (PD), and Huntington's disease (HD) (122). Our results showed that H<sub>2</sub>O<sub>2</sub> ACM induced the increasing of intracellular ROS and decreasing of MMP. These results are in line with recent data showing that mitochondria in microglial activation induced by LPS changes in their morphology which prominent elongated, needle-like and increases the number of microglial mitochondrial profiles (123).

All of these results might be imply that activated microglia with iron accumulation induced by H<sub>2</sub>O<sub>2</sub> ACM were shown profiles like microglia in neurodegenerative diseases, including increased proinflammatory cytokines, iron homeostasis alteration, and mitochondria dysfunction.

In summary, we studied the effect of oxidative stress to iron accumulation and microglial activation by exposing in the directly oxidative stress and the indirectly oxidative stress via ACM. Our data demonstrated that the indirectly oxidative stress via ACM induced iron accumulation and microglial activation which altered iron homeostasis proteins. This is the first study showing the increase of iron accumulation in the activated microglia which established by the concept of oxidative stress and glial cell interaction. These findings could be a better understanding of activated microglia. Furthermore, the correlations in age-related neurodegenerative diseases are needed to determine, which might be beneficial to find a therapeutic approach.



## REFERENCES

1. Colonna M, Butovsky O. Microglia Function in the Central Nervous System During Health and Neurodegeneration. *Annual review of immunology*. 2017;35:441-68.
2. Liu W, Tang Y, Feng J. Cross talk between activation of microglia and astrocytes in pathological conditions in the central nervous system. *Life sciences*. 2011;89(5-6):141-6.
3. Mairuae N, Connor JR, Cheepsunthorn P. Increased cellular iron levels affect matrix metalloproteinase expression and phagocytosis in activated microglia. *Neuroscience letters*. 2011;500(1):36-40.
4. Rathnasamy G, Ling E, Kaur C. Consequences of Iron Accumulation in Microglia and its Implications in Neuropathological Conditions. *CNS & neurological disorders drug targets*. 2013;12.
5. Xu H, Wang Y, Song N, Wang J, Jiang H, Xie J. New Progress on the Role of Glia in Iron Metabolism and Iron-Induced Degeneration of Dopamine Neurons in Parkinson's Disease. *Frontiers in molecular neuroscience*. 2017;10:455.
6. Hou Y, Dan X, Babbar M, Wei Y, Hasselbalch SG, Croteau DL, et al. Ageing as a risk factor for neurodegenerative disease. *Nat Rev Neurol*. 2019;15(10):565-81.
7. Thakur MK, Rattan SI. *Brain aging and therapeutic interventions*: Springer; 2012.
8. Taki Y, Thyreau B, Kinomura S, Sato K, Goto R, Kawashima R, et al. Correlations among brain gray matter volumes, age, gender, and hemisphere in healthy individuals. *PLoS one*. 2011;6(7):e22734.
9. Berti V, Mosconi L, Glodzik L, Li Y, Murray J, De Santi S, et al. Structural brain changes in normal individuals with a maternal history of Alzheimer's. *Neurobiology of aging*. 2011;32(12):2325.e17-26.
10. Wong T. Aging of the Cerebral Cortex. *McGill J Med*. 2002;6.
11. Dickstein DL, Kabaso D, Rocher AB, Luebke JI, Wearne SL, Hof PR. Changes in the structural complexity of the aged brain. *Aging cell*. 2007;6(3):275-84.
12. Hedden T, Gabrieli JD. Insights into the ageing mind: a view from cognitive neuroscience. *Nat Rev Neurosci*. 2004;5(2):87-96.

13. Park DC, Gutchess AH. Cognitive aging and everyday life. *Cognitive aging: A primer*. New York, NY, US: Psychology Press; 2000. p. 217-32.
14. Reuter-Lorenz P, Sylvester C-Y. The Cognitive Neuroscience of Working Memory and Aging. *Cognitive Neuroscience of Aging: Linking cognitive and cerebral aging*. 2005.
15. Yousem DM, Maldjian JA, Hummel T, Alsop DC, Geckle RJ, Kraut MA, et al. The effect of age on odor-stimulated functional MR imaging. *AJNR American journal of neuroradiology*. 1999;20(4):600-8.
16. Ota M, Yasuno F, Ito H, Seki C, Nozaki S, Asada T, et al. Age-related decline of dopamine synthesis in the living human brain measured by positron emission tomography with L-[beta-11C]DOPA. *Life sciences*. 2006;79(8):730-6.
17. Mattson MP, Maudsley S, Martin B. BDNF and 5-HT: a dynamic duo in age-related neuronal plasticity and neurodegenerative disorders. *Trends in neurosciences*. 2004;27(10):589-94.
18. Šimić G, Kostović I, Winblad B, Bogdanović N. Volume and number of neurons of the human hippocampal formation in normal aging and Alzheimer's disease. 1997;379(4):482-94.
19. Fabricius K, Jacobsen JS, Pakkenberg B. Effect of age on neocortical brain cells in 90+ year old human females—a cell counting study. *Neurobiology of aging*. 2013;34(1):91-9.
20. Pelvig DP, Pakkenberg H, Stark AK, Pakkenberg B. Neocortical glial cell numbers in human brains. *Neurobiology of aging*. 2008;29(11):1754-62.
21. Cotrina ML, Nedergaard M. Astrocytes in the aging brain. *Journal of neuroscience research*. 2002;67(1):1-10.
22. Lynch AM, Murphy KJ, Deighan BF, O'Reilly J-A, Gun'ko YK, Cowley TR, et al. The impact of glial activation in the aging brain. *Aging Dis*. 2010;1(3):262-78.
23. Finch CE. Neurons, glia, and plasticity in normal brain aging. *Neurobiology of aging*. 2003;24 Suppl 1:S123-7; discussion S31.
24. Perry VH, Matyszak MK, Fearn S. Altered antigen expression of microglia in the aged rodent CNS. *Glia*. 1993;7(1):60-7.
25. Sheffield LG, Berman NE. Microglial expression of MHC class II increases in normal aging of nonhuman primates. *Neurobiology of aging*. 1998;19(1):47-55.

26. Soreq L, Consortium UK, Consortium N, Rose J, Soreq E, Hardy J, et al. Major Shifts in Glial Regional Identity Are a Transcriptional Hallmark of Human Brain Aging. *Cell Reports*. 2016;18:557–70.
27. Pirpamer L, Hofer E, Gesierich B, De Guio F, Freudenberger P, Seiler S, et al. Determinants of iron accumulation in the normal aging brain. *Neurobiology of aging*. 2016;43:149-55.
28. Smith MA, Zhu X, Tabaton M, Liu G, McKeel DW, Jr., Cohen ML, et al. Increased iron and free radical generation in preclinical Alzheimer disease and mild cognitive impairment. *Journal of Alzheimer's disease : JAD*. 2010;19(1):363-72.
29. Floyd RA, Hensley K. Oxidative stress in brain aging. Implications for therapeutics of neurodegenerative diseases. *Neurobiology of aging*. 2002;23(5):795-807.
30. Mariani E, Polidori MC, Cherubini A, Mecocci P. Oxidative stress in brain aging, neurodegenerative and vascular diseases: an overview. *Journal of chromatography B, Analytical technologies in the biomedical and life sciences*. 2005;827(1):65-75.
31. Floyd RA. Antioxidants, oxidative stress, and degenerative neurological disorders. *Proceedings of the Society for Experimental Biology and Medicine Society for Experimental Biology and Medicine (New York, NY)*. 1999;222(3):236-45.
32. Singh A, Kukreti R, Saso L, Kukreti S. Oxidative Stress: A Key Modulator in Neurodegenerative Diseases. *Molecules*. 2019;24(8):1583.
33. Dei R, Takeda A, Niwa H, Li M, Nakagomi Y, Watanabe M, et al. Lipid peroxidation and advanced glycation end products in the brain in normal aging and in Alzheimer's disease. *Acta neuropathologica*. 2002;104(2):113-22.
34. Mecocci P, MacGarvey U, Kaufman AE, Koontz D, Shoffner JM, Wallace DC, et al. Oxidative damage to mitochondrial DNA shows marked age-dependent increases in human brain. *Annals of neurology*. 1993;34(4):609-16.
35. Smith CD, Carney JM, Starke-Reed PE, Oliver CN, Stadtman ER, Floyd RA, et al. Excess brain protein oxidation and enzyme dysfunction in normal aging and in Alzheimer disease. *Proceedings of the National Academy of Sciences of the United States of America*. 1991;88(23):10540-3.
36. Lushchak VI. Free radicals, reactive oxygen species, oxidative stress and its classification. *Chemico-biological interactions*. 2014;224:164-75.

37. Zhang X, Rosenstein BS, Wang Y, Lebowitz M, Wei H. Identification of possible reactive oxygen species involved in ultraviolet radiation-induced oxidative DNA damage. *Free radical biology & medicine*. 1997;23(7):980-5.
38. Mani S. Production of Reactive Oxygen Species and Its Implication in Human Diseases. In: Rani V, Yadav UCS, editors. *Free Radicals in Human Health and Disease*. New Delhi: Springer India; 2015. p. 3-15.
39. Kim GH, Kim JE, Rhie SJ, Yoon S. The Role of Oxidative Stress in Neurodegenerative Diseases. *Exp Neurobiol*. 2015;24(4):325-40.
40. Presnell CE, Bhatti G, Numan LS, Lerche M, Alkhateeb SK, Ghalib M, et al. Computational insights into the role of glutathione in oxidative stress. *Current neurovascular research*. 2013;10(2):185-94.
41. Song J, Kang SM, Lee WT, Park KA, Lee KM, Lee JE. Glutathione protects brain endothelial cells from hydrogen peroxide-induced oxidative stress by increasing nrf2 expression. *Exp Neurobiol*. 2014;23(1):93-103.
42. Dasuri K, Zhang L, Keller JN. Oxidative stress, neurodegeneration, and the balance of protein degradation and protein synthesis. *Free radical biology & medicine*. 2013;62:170-85.
43. Moos T. Brain iron homeostasis. *Danish medical bulletin*. 2002;49(4):279-301.
44. Benkovic SA, Connor JR. Ferritin, transferrin, and iron in selected regions of the adult and aged rat brain. *The Journal of comparative neurology*. 1993;338(1):97-113.
45. Connor JR, Snyder BS, Beard JL, Fine RE, Mufson EJ. Regional distribution of iron and iron-regulatory proteins in the brain in aging and Alzheimer's disease. *Journal of neuroscience research*. 1992;31(2):327-35.
46. Smith MA, Harris PL, Sayre LM, Perry G. Iron accumulation in Alzheimer disease is a source of redox-generated free radicals. *Proceedings of the National Academy of Sciences of the United States of America*. 1997;94(18):9866-8.
47. Singh N, Haldar S, Tripathi AK, Horback K, Wong J, Sharma D, et al. Brain iron homeostasis: from molecular mechanisms to clinical significance and therapeutic opportunities. *Antioxid Redox Signal*. 2014;20(8):1324-63.
48. Nnah IC, Wessling-Resnick M. Brain Iron Homeostasis: A Focus on Microglial Iron. *Pharmaceuticals (Basel)*. 2018;11(4):129.

49. Quintana C, Bellefquih S, Laval JY, Guerquin-Kern JL, Wu TD, Avila J, et al. Study of the localization of iron, ferritin, and hemosiderin in Alzheimer's disease hippocampus by analytical microscopy at the subcellular level. *Journal of Structural Biology*. 2006;153(1):42-54.
50. Arosio P, Ingrassia R, Cavadini P. Ferritins: a family of molecules for iron storage, antioxidation and more. *Biochimica et biophysica acta*. 2009;1790(7):589-99.
51. Connor JR, Menzies SL. Cellular management of iron in the brain. *Journal of the neurological sciences*. 1995;134 Suppl:33-44.
52. Moos T, Morgan EH. The metabolism of neuronal iron and its pathogenic role in neurological disease: review. *Annals of the New York Academy of Sciences*. 2004;1012:14-26.
53. Zecca L, Youdim MB, Riederer P, Connor JR, Crichton RR. Iron, brain ageing and neurodegenerative disorders. *Nat Rev Neurosci*. 2004;5(11):863-73.
54. Rouault TA. Iron metabolism in the CNS: implications for neurodegenerative diseases. *Nature Reviews Neuroscience*. 2013;14(8):551-64.
55. Zhang D-L, Ghosh MC, Rouault TA. The physiological functions of iron regulatory proteins in iron homeostasis - an update. *Front Pharmacol*. 2014;5:124-.
56. Zhou ZD, Tan E-K. Iron regulatory protein (IRP)-iron responsive element (IRE) signaling pathway in human neurodegenerative diseases. *Molecular Neurodegeneration*. 2017;12(1):75.
57. Liu J-L, Fan Y-G, Yang Z-S, Wang Z-Y, Guo C. Iron and Alzheimer's Disease: From Pathogenesis to Therapeutic Implications. *Frontiers in Neuroscience*. 2018;12:632.
58. Silmi AS. Iron Metabolism and Storage 2012 [cited 2020 20/03/2020]. Available from: <https://slideplayer.com/slide/12720658/>.
59. Ginhoux F, Greter M, Leboeuf M, Nandi S, See P, Gokhan S, et al. Fate mapping analysis reveals that adult microglia derive from primitive macrophages. *Science (New York, NY)*. 2010;330(6005):841-5.
60. Schulz C, Gomez Perdiguero E, Chorro L, Szabo-Rogers H, Cagnard N, Kierdorf K, et al. A lineage of myeloid cells independent of Myb and hematopoietic stem cells. *Science (New York, NY)*. 2012;336(6077):86-90.
61. Li Q, Barres BA. Microglia and macrophages in brain homeostasis and disease.

Nat Rev Immunol. 2018;18(4):225-42.

62. Paolicelli RC, Bolasco G, Pagani F, Maggi L, Scianni M, Panzanelli P, et al. Synaptic Pruning by Microglia Is Necessary for Normal Brain Development. *Science (New York, NY)*. 2011;333(6048):1456.

63. Tong L, Prieto GA, Kramar EA, Smith ED, Cribbs DH, Lynch G, et al. Brain-derived neurotrophic factor-dependent synaptic plasticity is suppressed by interleukin-1beta via p38 mitogen-activated protein kinase. *The Journal of neuroscience : the official journal of the Society for Neuroscience*. 2012;32(49):17714-24.

64. Lynch MA. Neuroinflammatory changes negatively impact on LTP: A focus on IL-1beta. *Brain research*. 2015;1621:197-204.

65. Kato G, Inada H, Wake H, Akiyoshi R, Miyamoto A, Eto K, et al. Microglial Contact Prevents Excess Depolarization and Rescues Neurons from Excitotoxicity. *eNeuro*. 2016;3(3).

66. Nedergaard M, Ransom B, Goldman SA. New roles for astrocytes: redefining the functional architecture of the brain. *Trends in neurosciences*. 2003;26(10):523-30.

67. Haydon PG, Carmignoto G. Astrocyte control of synaptic transmission and neurovascular coupling. *Physiological reviews*. 2006;86(3):1009-31.

68. Davalos D, Grutzendler J, Yang G, Kim JV, Zuo Y, Jung S, et al. ATP mediates rapid microglial response to local brain injury in vivo. *Nature neuroscience*. 2005;8(6):752-8.

69. Lee M, Schwab C, McGeer PL. Astrocytes are GABAergic cells that modulate microglial activity. *Glia*. 2011;59(1):152-65.

70. Norden DM, Fenn AM, Dugan A, Godbout JP. TGFbeta produced by IL-10 redirected astrocytes attenuates microglial activation. *Glia*. 2014;62(6):881-95.

71. Min KJ, Yang MS, Kim SU, Jou I, Joe EH. Astrocytes induce hemoxygenase-1 expression in microglia: a feasible mechanism for preventing excessive brain inflammation. *The Journal of neuroscience : the official journal of the Society for Neuroscience*. 2006;26(6):1880-7.

72. Sanagi T, Yuasa S, Nakamura Y, Suzuki E, Aoki M, Warita H, et al. Appearance of phagocytic microglia adjacent to motoneurons in spinal cord tissue from a presymptomatic transgenic rat model of amyotrophic lateral sclerosis. *Journal of*

neuroscience research. 2010;88(12):2736-46.

73. Saijo K, Glass CK. Microglial cell origin and phenotypes in health and disease. *Nat Rev Immunol*. 2011;11(11):775-87.

74. Van Ginderachter JA, Movahedi K, Hassanzadeh Ghassabeh G, Meerschaut S, Beschin A, Raes G, et al. Classical and alternative activation of mononuclear phagocytes: picking the best of both worlds for tumor promotion. *Immunobiology*. 2006;211(6-8):487-501.

75. Takeuchi H, Jin S, Wang J, Zhang G, Kawanokuchi J, Kuno R, et al. Tumor necrosis factor-alpha induces neurotoxicity via glutamate release from hemichannels of activated microglia in an autocrine manner. *The Journal of biological chemistry*. 2006;281(30):21362-8.

76. Neher JJ, Neniskyte U, Zhao JW, Bal-Price A, Tolkovsky AM, Brown GC. Inhibition of microglial phagocytosis is sufficient to prevent inflammatory neuronal death. *Journal of immunology (Baltimore, Md : 1950)*. 2011;186(8):4973-83.

77. Block ML, Hong JS. Microglia and inflammation-mediated neurodegeneration: multiple triggers with a common mechanism. *Progress in neurobiology*. 2005;76(2):77-98.

78. Nakamura Y. Regulating Factors for Microglial Activation. *Biological and Pharmaceutical Bulletin*. 2002;25(8):945-53.

79. Moss DW, Bates TE. Activation of murine microglial cell lines by lipopolysaccharide and interferon- $\gamma$  causes NO-mediated decreases in mitochondrial and cellular function. *European Journal of Neuroscience*. 2001;13(3):529-38.

80. Kato TA, Monji A, Yasukawa K, Mizoguchi Y, Horikawa H, Seki Y, et al. Aripiprazole inhibits superoxide generation from phorbol-myristate-acetate (PMA)-stimulated microglia in vitro: Implication for antioxidative psychotropic actions via microglia. *Schizophrenia Research*. 2011;129(2):172-82.

81. Maezawa I, Zimin PI, Wulff H, Jin LW. Amyloid-beta protein oligomer at low nanomolar concentrations activates microglia and induces microglial neurotoxicity. *The Journal of biological chemistry*. 2011;286(5):3693-706.

82. Streit WJ, Hurley SD, McGraw TS, Semple-Rowland SL. Comparative evaluation

of cytokine profiles and reactive gliosis supports a critical role for interleukin-6 in neuron-glia signaling during regeneration. *Journal of neuroscience research*. 2000;61(1):10-20.

83. Nakajima K, Kohsaka S. Microglia: Activation and Their Significance in the Central Nervous System. *The Journal of Biochemistry*. 2001;130(2):169-75.

84. Block ML, Zecca L, Hong JS. Microglia-mediated neurotoxicity: uncovering the molecular mechanisms. *Nat Rev Neurosci*. 2007;8(1):57-69.

85. Rouault TA, Cooperman S. Brain iron metabolism. *Seminars in pediatric neurology*. 2006;13(3):142-8.

86. McCarthy RC, Kosman DJ. Iron transport across the blood-brain barrier: development, neurovascular regulation and cerebral amyloid angiopathy. *Cellular and molecular life sciences : CMLS*. 2015;72(4):709-27.

87. Wang J, Song N, Jiang H, Wang J, Xie J. Pro-inflammatory cytokines modulate iron regulatory protein 1 expression and iron transportation through reactive oxygen/nitrogen species production in ventral mesencephalic neurons. *Biochimica et biophysica acta*. 2013;1832(5):618-25.

88. Thomsen MS, Andersen MV, Christoffersen PR, Jensen MD, Lichota J, Moos T. Neurodegeneration with inflammation is accompanied by accumulation of iron and ferritin in microglia and neurons. *Neurobiology of disease*. 2015;81:108-18.

89. Holland R, McIntosh AL, Finucane OM, Mela V, Rubio-Araiz A, Timmons G, et al. Inflammatory microglia are glycolytic and iron retentive and typify the microglia in APP/PS1 mice. *Brain, behavior, and immunity*. 2018;68:183-96.

90. Urrutia P, Aguirre P, Esparza A, Tapia V, Mena NP, Arredondo M, et al. Inflammation alters the expression of DMT1, FPN1 and hepcidin, and it causes iron accumulation in central nervous system cells. *Journal of neurochemistry*. 2013;126(4):541-9.

91. McCarthy RC, Sosa JC, Gardeck AM, Baez AS, Lee C-H, Wessling-Resnick M. Inflammation-induced iron transport and metabolism by brain microglia. *The Journal of biological chemistry*. 2018;293(20):7853-63.

92. Kumar V, Sami N, Kashav T, Islam A, Ahmad F, Hassan MI. Protein aggregation and neurodegenerative diseases: From theory to therapy. *European Journal of*



Medicinal Chemistry. 2016;124:1105-20.

93. Subhramanyam CS, Wang C, Hu Q, Dheen ST. Microglia-mediated neuroinflammation in neurodegenerative diseases. *Seminars in Cell & Developmental Biology*. 2019;94:112-20.

94. Perry VH, Nicoll JA, Holmes C. Microglia in neurodegenerative disease. *Nat Rev Neurol*. 2010;6(4):193-201.

95. Hirayama T, Nagasawa H. Chemical tools for detecting Fe ions. *J Clin Biochem Nutr*. 2017;60(1):39-48.

96. Tenopoulou M, Kurz T, Doulias P-T, Galaris D, Brunk UT. Does the calcein-AM method assay the total cellular 'labile iron pool' or only a fraction of it? *Biochem J*. 2007;403(2):261-6.

97. [cited 2020 20/03/2020]. Available from: [https://www.gbiosciences.com/Bioassays/Cell\\_Health\\_Assay/REDOX\\_Probes/DCFH-DA-Redox\\_Probe](https://www.gbiosciences.com/Bioassays/Cell_Health_Assay/REDOX_Probes/DCFH-DA-Redox_Probe).

98. Bouvier DS, Jones EV, Quesseveur G, Davoli MA, T AF, Quirion R, et al. High Resolution Dissection of Reactive Glial Nets in Alzheimer's Disease. *Scientific reports*. 2016;6:24544.

99. Lopes KO, Sparks DL, Streit WJ. Microglial dystrophy in the aged and Alzheimer's disease brain is associated with ferritin immunoreactivity. *Glia*. 2008;56(10):1048-60.

100. Mehlhase J, Gieche J, Widmer R, Grune T. Ferritin levels in microglia depend upon activation: Modulation by reactive oxygen species. *Biochimica et biophysica acta*. 2006;1763:854-9.

101. Kaneko Y, Kitamoto T, Tateishi J, Yamaguchi K. Ferritin immunohistochemistry as a marker for microglia. *Acta neuropathologica*. 1989;79(2):129-36.

102. Cheepsunthorn P, Palmer C, Connor JR. Cellular distribution of ferritin subunits in postnatal rat brain. *Journal of Comparative Neurology*. 1998;400(1):73-86.

103. Lee PL, Gelbart T, West C, Halloran C, Beutler E. The human Nramp2 gene: characterization of the gene structure, alternative splicing, promoter region and polymorphisms. *Blood cells, molecules & diseases*. 1998;24(2):199-215.

104. Wang Y, Xu E, Musich PR, Lin F. Mitochondrial dysfunction in neurodegenerative diseases and the potential countermeasure. *CNS Neuroscience & Therapeutics*.

2019;25(7):816-24.

105. Nakamura Y. Regulating factors for microglial activation. *Biological & pharmaceutical bulletin*. 2002;25(8):945-53.

106. Quincozes-Santos A, Bobermin LD, Latini A, Wajner M, Souza DO, Gonçalves CA, et al. Resveratrol protects C6 astrocyte cell line against hydrogen peroxide-induced oxidative stress through heme oxygenase 1. *PloS one*. 2013;8(5):e64372.

107. Kuno R, Wang J, Kawanokuchi J, Takeuchi H, Mizuno T, Suzumura A. Autocrine activation of microglia by tumor necrosis factor- $\alpha$ . *J Neuroimmunol*. 2005;162(1-2):89-96.

108. Brás JP, Bravo J, Freitas J, Barbosa MA, Santos SG, Summavielle T, et al. TNF- $\alpha$ -induced microglia activation requires miR-342: impact on NF- $\kappa$ B signaling and neurotoxicity. *Cell Death & Disease*. 2020;11(6):415.

109. Jha MK, Jo M, Kim JH, Suk K. Microglia-Astrocyte Crosstalk: An Intimate Molecular Conversation. *The Neuroscientist : a review journal bringing neurobiology, neurology and psychiatry*. 2019;25(3):227-40.

110. Kim JH, Ko PW, Lee HW, Jeong JY, Lee MG, Kim JH, et al. Astrocyte-derived lipocalin-2 mediates hippocampal damage and cognitive deficits in experimental models of vascular dementia. *Glia*. 2017;65(9):1471-90.

111. di Penta A, Moreno B, Reix S, Fernandez-Diez B, Villanueva M, Errea O, et al. Oxidative stress and proinflammatory cytokines contribute to demyelination and axonal damage in a cerebellar culture model of neuroinflammation. *PloS one*. 2013;8(2):e54722-e.

112. Dello Russo C, Cappoli N, Coletta I, Mezzogori D, Paciello F, Pozzoli G, et al. The human microglial HMC3 cell line: where do we stand? A systematic literature review. *Journal of neuroinflammation*. 2018;15(1):259.

113. Hjorth E, Zhu M, Toro VC, Vedin I, Palmblad J, Cederholm T, et al. Omega-3 fatty acids enhance phagocytosis of Alzheimer's disease-related amyloid-beta<sub>42</sub> by human microglia and decrease inflammatory markers. *Journal of Alzheimer's disease : JAD*. 2013;35(4):697-713.

114. Nagai A, Nakagawa E, Hatori K, Choi HB, McLarnon JG, Lee MA, et al. Generation and characterization of immortalized human microglial cell lines: expression of

cytokines and chemokines. *Neurobiology of disease*. 2001;8(6):1057-68.

115. Ott L, Resing K, Sizemore A, Heyen J, Cocklin R, Pedrick N, et al. Tumor Necrosis Factor- $\alpha$ - and Interleukin-1-Induced Cellular Responses: Coupling Proteomic and Genomic Information. *J Proteome Res*. 2011;10.

116. Connor JR, editor Cellular and regional maintenance of iron homeostasis in the brain: normal and diseased states. *Iron in Central Nervous System Disorders*; 1993 1993//; Vienna: Springer Vienna.

117. Connor JR, Boeshore KL, Benkovic SA, Menzies SL. Isoforms of ferritin have a specific cellular distribution in the brain. *Journal of neuroscience research*. 1994;37(4):461-5.

118. Connor JR, Snyder BS, Arosio P, Loeffler DA, LeWitt P. A quantitative analysis of isoforms of ferritin in select regions of aged, parkinsonian, and Alzheimer's diseased brains. *Journal of neurochemistry*. 1995;65(2):717-24.

119. Rathore KI, Redensek A, David S. Iron homeostasis in astrocytes and microglia is differentially regulated by TNF- $\alpha$  and TGF- $\beta$ 1. *Glia*. 2012;60(5):738-50.

120. Hubert N, Hentze MW. Previously uncharacterized isoforms of divalent metal transporter (DMT)-1: Implications for regulation and cellular function. *Proceedings of the National Academy of Sciences*. 2002;99(19):12345.

121. Ingrassia R, Garavaglia B, Memo M. DMT1 Expression and Iron Levels at the Crossroads Between Aging and Neurodegeneration. 2019;13(575).

122. Zorova LD, Popkov VA, Plotnikov EY, Silachev DN, Pevzner IB, Jankauskas SS, et al. Mitochondrial membrane potential. *Analytical biochemistry*. 2018;552:50-9.

123. Banati RB, Egensperger R, Maassen A, Hager G, Kreutzberg GW, Graeber MB. Mitochondria in activated microglia in vitro. *Journal of neurocytology*. 2004;33(5):535-41.



APPENDICES

จุฬาลงกรณ์มหาวิทยาลัย  
**CHULALONGKORN UNIVERSITY**

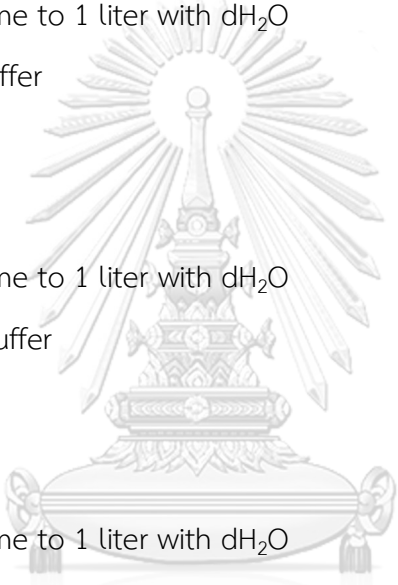
## APPENDIX

### SPECIFIC BUFFER AND REAGENTS

1. Dulbecco's modified Eagle's medium (DMEM) stock medium 1 liter
  - Sodium Pyruvate powder 110 mg
  - Sodium bicarbonate 3.7 g
  - Penicillin-Streptomycin solution 10 ml
  - HEPES, free acid 10 ml
  - Sterilized by filtering through a 0.2  $\mu$ m membrane filter
  - Store at 4 °C
2. 10X Phosphate Buffered Saline (PBS) 1 liter
  - Phosphate Buffered Saline powdered
  - Add ddH<sub>2</sub>O up to 1 liter and sterilize by autoclaving
3. 1X Phosphate Buffered Saline (PBS) 1 liter
  - 10X Phosphate Buffered Saline 100 ml
  - Add ddH<sub>2</sub>O up to 1 liter and sterilize by autoclaving
4. Sodium dodecyl sulfate-polyacrylamide gel electrophoresis (SDS–PAGE) preparations

Reagents	Separating gel (ml)		4% Stacking gel (ml)
	10%	12%	
H <sub>2</sub> O	4	3.25	4.08
30% Acrylamide	3.3	4	1.02
1.5 M Tris (pH 8.8)	2.5	2.5	-
1.0 M Tris (pH 6.8)	-	-	0.75
10% SDS	100 $\mu$ l	100 $\mu$ l	60 $\mu$ l
10% APS	100 $\mu$ l	100 $\mu$ l	60 $\mu$ l
TEMED	10 $\mu$ l	10 $\mu$ l	6 $\mu$ l
<b>Total volume (ml)</b>	<b>10 ml</b>	<b>10 ml</b>	<b>6 ml</b>

5. 1.5 M Tris base (pH 8.8) 100 ml
- Tris base 18.171 g
  - dH<sub>2</sub>O 80 ml
  - Adjust the pH to 8.8 with conc. HCl and conc. NaOH
  - Adjust the volume to 100 ml with dH<sub>2</sub>O
6. 1 M Tris base (pH 6.8) 100 ml
- Tris base 12.14 g
  - dH<sub>2</sub>O 80 ml
  - Adjust the pH to 6.8 with conc. HCl and conc. NaOH
  - Adjust the volume to 100 ml with dH<sub>2</sub>O
7. 0.5 M Tris HCl 100 ml
- Tris base 6 g
  - dH<sub>2</sub>O 40 ml
  - Adjust the pH to 6.8 with conc. HCl
  - Adjust the volume to 100 ml with dH<sub>2</sub>O
8. 10% SDS 100 ml
- SDS 10 g
  - Adjust the volume to 100 ml with dH<sub>2</sub>O
9. 10% APS 1 ml
- APS 0.1 g
  - Adjust the volume to 1 ml with dH<sub>2</sub>O
10. 5X running buffer 1 liter
- Tris base 15.1 g
  - Glycine 94 g
  - SDS 5 g
  - Adjust the volume to 1 liter with dH<sub>2</sub>O



11. 10X transfer buffer	1 liter
— Tris base	30 g
— Glycine	144 g
— Adjust the volume to 1 liter with dH <sub>2</sub> O	
12. 1X transfer buffer	1 liter
— 10X transfer buffer	100 ml
— Methanol	100 ml
— Adjust the volume to 1 liter with dH <sub>2</sub> O	
13. 10X TBS washing buffer	1 liter
— Tris base	24.2 g
— NaCl	80 g
— Adjust the volume to 1 liter with dH <sub>2</sub> O	
14. 1X TBS-T washing buffer	1 liter
— 10X TBS	100 ml
— Tween 20	1 ml
— Adjust the volume to 1 liter with dH <sub>2</sub> O	
15. Blocking buffer	50 ml
— 5% Skim milked	25 g
— 1X TBS-T	50 ml
16. 10% Neutral Buffered Formalin (NBF)	100 ml
— 37% Formaldehyde	10 ml
— dH <sub>2</sub> O	90 ml
— Na <sub>2</sub> HPO <sub>4</sub>	650 mg
— NaH <sub>2</sub> PO <sub>4</sub>	400 mg
17. Reaction mix for cDNA synthesis	
— 5X Reaction buffer	4 μl
— Oligo dT	1 μl

– Revert Aid	1 $\mu$ l
– Ribolock	1 $\mu$ l
– 10mM dNTP	2 $\mu$ l
– 2 $\mu$ g of RNA + RNase free water	11 $\mu$ l
– Total volume	20 $\mu$ l

## 18. Reaction mix for PCR

– RNase free water	7.15 $\mu$ l
– (10X) PCR buffer	1 $\mu$ l
– dNTP (10mM)	0.2 $\mu$ l
– 50mM MgCl <sub>2</sub>	0.2 $\mu$ l
– Taq pol	0.05 $\mu$ l
– Forward primer	0.2 $\mu$ l
– Reward primer	0.2 $\mu$ l
– Sample (cDNA)	1 $\mu$ l
– Total volume	10 $\mu$ l

## 19. Reaction mix for q-PCR

– RNase free water	5 $\mu$ l
– SYBR Green	2 $\mu$ l
– Forward primer	1 $\mu$ l
– Reward primer	1 $\mu$ l
– Sample (cDNA)	1 $\mu$ l
– Total volume	10 $\mu$ l





## VITA

**NAME** Rattanakorn Suntawalimp

**DATE OF BIRTH** 05 August 1993

**PLACE OF BIRTH** Bangkok, Thailand

**INSTITUTIONS ATTENDED** The Degree of Bachelor of Science (Occupational Therapy), Mahidol University

**HOME ADDRESS** 440 Soi Chareonkung 67 Yannawa Sathon Bangkok 10120

